Shape minimization of the dissipated energy in dyadic trees

Xavier Dubois de La Sablonière, Benjamin Mauroy, Yannick Privat

SHAPE MINIMIZATION OF THE DISSIPATED ENERGY IN DYADIC TREES

Xavier Dubois de La Sablonière[1, 2], Benjamin Mauroy[3] and Yannick Privat[1, 4]

Abstract. In this paper, we study the role of boundary conditions on the optimal shape of a dyadic tree crossed by a newtonian fluid. Our optimization problem consists in finding the shape of the tree that minimizes the viscous energy dissipated by the fluid with a constrained volume and with the condition that a given total flow crosses the tree. Two fluid regimes are studied: (i) low flow regime (Poiseuille) in trees with an arbitrary number of generations using a matricial approach and (ii) non linear flow regime (Navier-Stokes) in trees of two generations using shape derivatives in an augmented lagrangian algorithm coupled with a 2D/3D finite elements code to solve Navier-Stokes equations. It relies on the study of a finite dimensional optimization problem in the case (i) and on a shape optimization problem in the case (ii). We show that the optimal shape is highly dependant on the boundary conditions of the fluid applied at the leaves of the tree. Moreover our numerical results seem to indicate that the behavior of the non linear case is similar to that of the Poiseuille case, at least for moderate Reynolds number (around 100).

Résumé. Dans cet article, nous étudions le rôle des conditions au bord sur la forme optimale d'un arbre dichotomique traversé par un fluide newtonien. Notre problème d'optimisation consiste à déterminer la forme de l'arbre minimisant l'énergie visqueuse dissipée par le fluide, sous contraintes de volume prescrit et de flux total traversant l'arbre fixé. Deux régimes de fluide sont étudiés : (i) régime lent (Poiseuille) dans des arbres ayant un nombre de générations abitraire, en utilisant une approche matricielle et (ii) régime non linéaire (Navier-Stokes) dans des arbres ayant deux générations, en utilisant la dérivée par rapport au domaine dans un algorithme de Lagrangien augmenté couplé à un code d'éléments finis 2D/3D pour résoudre les équations de Navier-Stokes. Nous nous ramenons à l'étude d'un problème d'optimisation en dimension finie dans le cas (i) et à un problème d'optimisation de forme dans le cas (ii). Nous montrons que l'arbre optimal dépend fortement des conditions au bord imposées sur le fluide, en sortie de l'arbre. Par ailleurs, nos résultats numériques semblent indiquer que le comportement du cas non linéaire est similaire au cas Poiseuille, au moins pour des nombres de Reynolds modérés (de l'ordre de 100).

1991 Mathematics Subject Classification. 35Q30, 49K30, 65K10.

October 30, 2009.

Introduction and motivations

Tree structures are very common means to transport a product between two regions of different scales. These structures are often crossed by a fluid which acts as a transporter. The circulation of the fluid in such structures can be costly and the question of the optimization of the tree geometry arises.

Keywords and phrases: Shape optimization, Dyadic trees, Poiseuille's law, Fluid Mechanics, Stokes and Navier-Stokes systems.

[1] Université d'Orléans, Laboratoire MAPMO, CNRS, UMR 6628, Fédération Denis Poisson, FR 2964, Bat. Math., BP 6759, 45067 Orléans cedex 2, France

[2] SUPELEC, Plateau de Moulon, 91192 Gif-sur-Yvette, France ; e-mail: Xavier.Duboisdelasabloniere@supelec.fr

[3] Laboratoire MSC, Université Paris 7, CNRS, 10 rue Alice Domon et Léonie Duguet, F-75205 Paris cedex 13, France ; e-mail: Benjamin.Mauroy@univ-paris-diderot.fr

[4] IRMAR, ENS Cachan Bretagne, Univ. Rennes 1, CNRS, UEB, av. Robert Schuman, F-35170 Bruz, France ; e-mail: Yannick.Privat@bretagne.ens-cachan.fr

Important applications of this problem exist, like in industry, in the study of river basins, in water treatment or in biology and medicine. An answer, even partial, could help, for instance, to better understand organs like lungs or cardiovascular system. These two examples have to deal with energy dissipation due to air or blood circulation (see [28]). These organs are subject to dysfunctions which are often consequences of an increase of their hydrodynamical resistance and thus of a loss of efficiency of the geometrical structures as transport systems. Hence, dysfunctions like asthma or vascular accidet are often linked to an increase of the hydrodynamical resistance of the structure.

Thus, researching the optimal shapes of tree structures is an important problem. Preceding studies have been made on this topic in the past like in [3, 4, 16, 20, 27] each on particular situations and applications.

In this work, we look for the shape of dyadic trees that minimizise the viscous energy of a Newtonian fluid under a volume constraint. Such structures are indeed good candidates for the modelling of mammals bronchial trees [20]. In the first part of this paper, we study the case of low flow regime (Poiseuille flow) and we use a matricial formulation of the problem as in [12, 21]. In the second part, we study the case of non linear Navier-Stokes flow (Reynolds ~ 100) thanks to a numerical shape minimization method based on the use of shape derivatives (see [13, 24]). We show that the optimal structure depends on the fluid boundary conditions that are applied at tree root and leaves. Indeed, under the constraint that a given flow crosses the tree, the optimal shape is very different according to the conditions imposed at the leaves: Dirichlet conditions or strictly identical Neumann conditions lead to an optimal tree with particular relationships between the flow in a branch and its diameter; non identical Neumann conditions lead to a degenerated tree reduced to a tube and only one leaf remains accessible to the fluid from the root. Moreover the numerical simulations in the non linear case show similar behavior than for the low flow regime and give precisely the geometry of the bifurcation.

Note that we focus here on the 3D case, however it is easy to see, with very few changes in the reasoning, that our results would also hold for the 2D case.

In the following, we will call *inlet* of a dyadic tree either the open surface of the root of the tree or the root of the tree itself, depending on the context. Similarly, we will call *outlets* of a tree either the open surfaces of its leaves or its leaves themselves, also depending on the context. Mainly, we will refer to the open surfaces if we speak of boundary conditions and to the branches in the other cases. Note that this terminology does not mean necessarily that fluid is going in the tree through the inlet and out of the tree through the outlet.

1. The case of a fluid driven by Poiseuille's law: a theoretical result

We will use the following notations throughout this section:

$[x]$, with $x \in \mathbb{R}$	the integer part of x
$B^\top$, where B is a matrix	the transpose of B
$(\boldsymbol{e_1}, \dots, \boldsymbol{e_n})$, with $n \in \mathbb{N}^*$	the standard basis of $\mathbb{R}$
$\langle \boldsymbol{x}, \boldsymbol{y} \rangle$, where $\boldsymbol{x}$ and $\boldsymbol{y}$ are two vectors with same length	the euclidean inner product
$\|.\|$	the euclidian norm, induced by the inner product $\langle ., . \rangle$
$\mathrm{diag}\boldsymbol{u}$, where $\boldsymbol{u} = (u_i)_{i \in [1,n]} \in \mathbb{R}^{n \times 1}$	the diagonal matrix $D = (d_{i,j})_{1 \leq i,j \leq n}$ such that $d_{i,i} = u_i$ for all $i \in [1, n]$.

1.1. The model

We introduce here all the models used in this article.

1.1.1. *Poiseuille's law*

We consider the incompressible flow of a viscous fluid (of dynamic viscosity $\mu > 0$) through a cylindrical rigid pipe whose length is $L > 0$ and radius is $R > 0$ in a steady and low regime. We impose a *no-slip* condition on

the lateral boundary. We refer the inlet to 0 and the outlet to 1. Pressures ($p_0 > 0$ and $p_1 > 0$) at its ends are supposed to be uniform over the section. The volumetric flow rate Φ is chosen positive if the flow goes from the section 0 to the section 1.
If we solve the Navier-Stokes equations which rule the flow of the fluid through the pipe, we obtain that the velocity profile is parabolic and we find Poiseuille's law. This law boils down to a linear relationship between the pressure drop $p_0 - p_1$ and the volumetric flow rate Φ through this pipe,

$$p_0 - p_1 = r\Phi$$

where

$$r = \frac{8\mu L}{\pi R^4} > 0.$$

Therefore, if the pressure drop $p_0 - p_1$ is positive, the flow goes from the section 0 to the section 1, which is physically relevant.
We can draw a comparison between this model and Ohm's law considering the pressure drop as a potential difference and the volumetric flow rate as a current. Then, the proportionality constant r could be defined as a hydrodynamic resistance. Moreover, assuming that the flow is incompressible, the flow rate is conserved through the pipe.

1.1.2. *The dyadic tree*

We consider the flow of an incompressible and viscous fluid whose dynamic viscosity is μ through a finite dyadic tree of $N+1$ generations ($N \in \mathbb{N}$, $N \geq 1$). We will consider that a new generation in this tree occurs when a bifurcation is created, so that we will say that the root branch corresponds to generation 1 and the ramified branches at the end of the tree to generation $N+1$. Nevertheless, we will make the distinction between the notion of generation and the notion of level in the tree. A level is a number associated to a generation, equal to 1 for generation 2 and increasing from 1 at each eneration. Therefore, a tree with $N+1$ generations has N levels. The use of levels makes the indexation of all the variables for our problem easier. They will be denoted in all this section by i.

Thus, this tree has 2^N outlets and $2^{N+1} - 1$ branches. This tree is composed of connected rigid cylindrical pipes through which the fluid follows Poiseuille's law. We assume that the volumetric flow rate $\Phi > 0$ which enters this tree and all the pressures at the outlets of the tree are fixed. They are considered as data for our problem.

Let us define the sets $\mathcal{B}_{N,i}$ of couples of indexes which locate each branch belonging to a given level i ($i \in [1, N]$)

$$\mathcal{B}_{N,i} := \left\{(i,j) \mid j \in [\![1, 2^i]\!]\right\}. \tag{1}$$

In other terms, i represents the level and j the position of the branch at this level. Thus, the set $\mathcal{B}_N$ composed of all the indexes locating the pipes of the overall tree is defined by

$$\mathcal{B}_N := \bigcup_{i \in [1,N]} \mathcal{B}_{N,i}. \tag{2}$$

Let us notice that this set does not include the root branch of the tree whose radius is $R_0 \in \mathbb{R}_+^*$, length $L_0 \in \mathbb{R}_+^*$, pressure at its inlet $p_0 \in \mathbb{R}_+^*$ (the pressure at the inlet of the overall tree) and pressure at its outlet $p_1 \in \mathbb{R}_+^*$. Thus, its hydrodynamic resistance is $r_0 := \frac{8\mu L_0}{\pi R_0^4}$. According to Poiseuille's law, one has

$$p_0 - p_1 = r_0\Phi.$$

For a given pipe located in the tree by the couple $(i,j) \in \mathcal{B}_N$, let us denote by $R_{i,j} > 0$ its radius and by $L_{i,j} > 0$ its length. Therefore, one can characterize this pipe by its hydrodynamic resistance $r_{i,j} := \dfrac{8\mu L_{i,j}}{\pi R_{i,j}^4}$.

Moreover, let $q_{i,j}$ and $p_{i,j} > 0$ be, respectively, the volumetric flow rate through this pipe and the pressure at its outlet. The flow rate $q_{i,j}$ is chosen positive if the flow goes from this pipe to its daughter pipes and negative else.

Then, we consider a pipe whose index is $(i,j) \in \bigcup_{i\in[1,N-1]} \mathcal{B}_{N,i}$. Since the tree is dyadic, the hydrodynamic resistances of its (two) daughter pipes are $r_{i+1,2j-1}$ and $r_{i+1,2j}$, which belong to the $(i+1)$-th level. Then, we define the ratios $x_{i+1,2j}$ and $x_{i+1,2j+1}$, representing the evolution of the geometry of the tree between the levels i and $i+1$ by

$$x_{i+1,2j-1} := \frac{r_{i,j}}{r_{i+1,2j-1}} = \frac{L_{i,j}}{L_{i+1,2j-1}} \left(\frac{R_{i+1,2j-1}}{R_{i,j}}\right)^4 \text{ and } x_{i+1,2j} := \frac{r_{i,j}}{r_{i+1,2j}} = \frac{L_{i,j}}{L_{i+1,2j}} \left(\frac{R_{i+1,2j}}{R_{i,j}}\right)^4. \tag{3}$$

Moreover, we assume that the ratio of reduction is the same for the radius and the length between a mother branch and its daughter, then

$$x_{i+1,2j-1} = \left(\frac{R_{i+1,2j-1}}{R_{i,j}}\right)^3 \text{ and } x_{i+1,2j} = \left(\frac{R_{i+1,2j}}{R_{i,j}}\right)^3. \tag{4}$$

Figure 1 shows an example of a dyadic tree and of our notations in the special case where N is equal to 2.

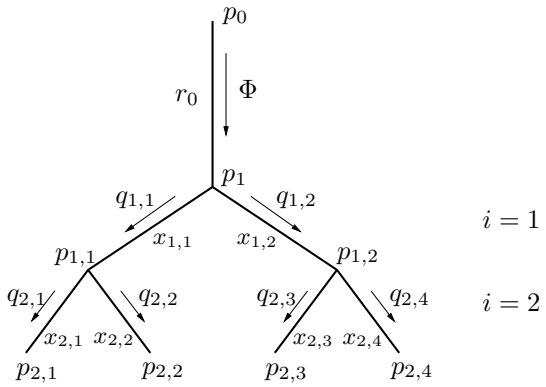

FIGURE 1. An example of dyadic tree with three generations ($N = 2$). Note that the flows $q_{i,j}$ can be either positive or negative ($(i,j) \in \mathcal{B}_N$).

With a view to establishing a relationship between the 2^N pressures and the 2^N volumetric rate flows at the outlets of the tree, we need to follow the fluid through paths in the tree. Therefore, one has to define the notions of path and subpath in the tree.

Definition 1.1. Notion of path and subpath.

(1) The path $\Pi_{0\to(i,j)}$ (with $(i,j) \in \mathcal{B}_N$) is the set of couples of indexes of the i branches needed to link the root branch denoted by 0 and the branch located by (i,j). It includes the branch denoted by (i,j) but not the root branch. More precisely,

$$\Pi_{0\to(i,j)} := \{(1,m_i), \ldots, (i-1,m_2), (i,m_1)\}, \tag{5}$$

where $(m_k)_{1\leq k\leq i}$ denotes the sequence of positive integers defined by

$$\left\{\begin{array}{l} m_1 = j \\ m_{k+1} = \left[\dfrac{m_k+1}{2}\right], \ \forall k \in [1, i-1]. \end{array}\right.$$

(2) Let $(i,j) \in \mathcal{B}_N$ and $s \in [0,i]$. For a given path $\Pi_{0\to(i,j)}$, the subpath $\Pi_{0\to(i,j)}(s)$ is the set of couples of indexes of the m branches needed to link the root branch and a branch located at the s-th level following a part of the path $\Pi_{0\to(i,j)}$. More precisely, the subpath $\Pi_{0\to(i,j)}(s)$ is the subset of $\Pi_{0\to(i,j)}$ defined by

$$\Pi_{0\to(i,j)}(s) := \left\{\begin{array}{ll} \{(1,m_i),\dots,(s,m_{i-s+1})\} & \text{if } s \geq 1 \\ \emptyset & \text{if } s = 0. \end{array}\right. \tag{6}$$

Thanks to this notion, one can make a change of variables, which will be very useful in the second part of this section, devoted to the optimization of a given criterion with respect to the geometry of the tree, represented by the $2^{N+1}-2$ variables $\{x_{i,j}\}_{(i,j)\in\mathcal{B}_N}$. From now on, we replace variables $x_{i,j}$ by $\xi_{i,j}$ defined by

$$\forall (i,j) \in \mathcal{B}_N, \ \xi_{i,j} := \prod_{(k,l)\in\Pi_{0\to(i,j)}} x_{k,l}. \tag{7}$$

It has to be noticed that the map $\{x_{i,j}\}_{(i,j)\in\mathcal{B}_N} \longmapsto \{\xi_{i,j}\}_{(i,j)\in\mathcal{B}_N}$ is obviously a C^1-diffeomorphism so that it defines a change of variable.
Moreover, $\frac{r_0}{\xi_{i,j}}$ represents the hydrodynamic resistance $r_{i,j}$ of the pipe denoted by (i,j).
For instance, in the case $N=2$ (see figure 1), the path linking the inlet to the first outlet is $\Pi_{0\to(2,1)} := \{(1,1);(2,1)\}$ and the geometric variables of theses branches are

$$x_{1,1} := \frac{r_0}{r_{1,1}} = \left(\frac{R_{1,1}}{R_0}\right)^3, \ \xi_{1,1} := x_{1,1}, \text{ and } x_{2,1} := \frac{r_0}{r_{2,1}} = \left(\frac{R_{2,1}}{R_0}\right)^3, \ \xi_{2,1} := x_{1,1}x_{1,2}.$$

Definition 1.2. Let us define:

- the vector $\boldsymbol{p}$ containing all the pressures at the outlets of the tree, *i.e.*

$$\boldsymbol{p} := (p_{N,1},\dots,p_{N,2^N})^\top \in (\mathbb{R}_+^*)^{2^N\times 1},$$

- the vector $\boldsymbol{q}$ containing all the volumetric flow rates crossing the leaves of the tree, *i.e.*

$$\boldsymbol{q} := (q_{N,1},\dots,q_{N,2^N})^\top \in \mathbb{R}^{2^N\times 1},$$

- the vector $\boldsymbol{\xi}$ representing the resistances of the tree, *i.e.*

$$\boldsymbol{\xi} := (\xi_{1,1},\xi_{1,2},\dots,\xi_{N,1},\dots,\xi_{N,2^N})^\top \in (\mathbb{R}_+^*)^{(2^{N+1}-2)\times 1}.$$

Definition 1.3. Given two positive integers i and j and their binary expressions

$$i = \sum_{k=0}^{\infty} \alpha_k 2^k, \ j = \sum_{k=0}^{\infty} \beta_k 2^k \text{ with } (\alpha_k,\beta_k) \in \{0,1\}^2, \ \forall k \in \mathbb{N},$$

we define $\nu_{i,j}$ as

$$\nu_{i,j} := \min\{k \in \mathbb{N}^* \mid \alpha_l = \beta_l, \forall l \geq k\}.$$

Thanks to Poiseuille's law, we are able to establish a linear relationship between the vectors $\boldsymbol{p}$ and $\boldsymbol{q}$.

Proposition 1.4. *Let $N \in \mathbb{N}^*$. One has*

$$p_0 \boldsymbol{u_N} - \boldsymbol{p} = A_N(\boldsymbol{\xi})\boldsymbol{q}, \tag{8}$$

where

- $A_N(\boldsymbol{\xi}) \in \mathbb{R}^{2^N \times 2^N}$ *is the resistance matrix of the tree, defined by*

$$A_N(\boldsymbol{\xi}) = (a^N_{i,j})_{1 \leq i,j \leq 2^N},\ a^N_{i,j} := \begin{cases} r_0 + \displaystyle\sum_{(k,l) \in \Pi_{0 \to (N,i)}(N - \nu_{i-1,j-1})} \frac{r_0}{\xi_{k,l}} & \text{if } \nu_{i-1,j-1} > 0 \\ r_0 & \text{if } \nu_{i-1,j-1} = 0 \end{cases} \tag{9}$$

- $\boldsymbol{u_N} \in \mathbb{R}^{2^N \times 1}$ *denotes the ones vector* i.e. $\boldsymbol{u_N} = (1, \ldots, 1)^\top$.

Remark 1.5. What is the meaning of $\Pi_{0 \to (N,i)}(N - \nu_{i-1,j-1})$? $\Pi_{0 \to (N,i)}(N - \nu_{i-1,j-1})$ is a subpath corresponding to the intersection of the two paths $\Pi_{0 \to (N,i)}$ and $\Pi_{0 \to (N,j)}$.

Proof. (see [12], where a close result is proved) The linearity of the relationship between $\boldsymbol{p}$ and $\boldsymbol{q}$ comes from Poiseuille's law. Hence it is sufficient to compute the pressure vectors $\boldsymbol{p}$ related to the elements of canonical basis of $\mathbb{R}^{2^N \times 1}$. Let us begin with $\boldsymbol{q} = (1, 0, \ldots, 0)^\top \in \mathbb{R}^{2^N \times 1}$. It boils down to the case in which the fluid exits the tree only by the outlet denoted by $(N, 1)$. In other terms, the fluid flows through the tree using the path $\Pi_{0 \to (N,1)}$. By conservation, the volumetric flow rate which enters the tree through the root branch is exactly $\Phi = 1$, so that the pressure p_1 at the outlet of the root branch is $p_0 - r_0$. As there is no flow in the right-hand subtree stemming from the root branch, the pressure at its outlets (whose couples of indexes are between $(N, 2^{N-1}+1)$ and $(N, 2^N)$) is the same as at the outlet of the root branch, namely $p_0 - r_0$. Similarly, the pressure $p_{1,1}$ at the outlet of the branch denoted by $(1, 1)$ is $p_0 - (r_0 + r_{1,1}) = p_0 - r_0\left(1 + \frac{1}{\xi_{1,1}}\right)$. Following this approach recursively, one finds pressures at the outlet of the branches of the path $\Pi_{0 \to (N,1)}$ denoted by $(i, 1)$ with $i \in [1, N]$ to be $p_0 - \left(r_0 + \displaystyle\sum_{(k,l) \in \Pi_{0 \to (N,1)}(i)} r_{k,l}\right) = p_0 - r_0\left(1 + \displaystyle\sum_{(k,l) \in \Pi_{0 \to (N,1)}(i)} \frac{1}{\xi_{k,l}}\right)$, respectively. Therefore, the pressure $p_{N,j}$ (with $j \in [\![1, 2^N]\!]$) at the outlets of the tree is $p_0 - r_0\left(1 + \displaystyle\sum_{(k,l) \in \Pi_{0 \to (N,1)}(N - \nu_{0,j-1})} \frac{1}{\xi_{k,l}}\right)$. Applying the same reasoning to any vector $\boldsymbol{q} = (0, \ldots, 0, 1, 0, \ldots, 0)^\top \in \mathbb{R}^{2^N \times 1}$ (with 1 at the i-th position) yields

$$\boldsymbol{p} = \left(p_0 - r_0\left(1 + \sum_{(k,l) \in \Pi_{0 \to (N,i)}(N - \nu_{i,0})} \frac{1}{\xi_{k,l}}\right), \ldots, p_0 - r_0\left(1 + \sum_{(k,l) \in \Pi_{0 \to (N,i)}(N - \nu_{i,2^N-1})} \frac{1}{\xi_{k,l}}\right)\right)^\top.$$

Consequently, we obtain

$$\forall i \in [\![1, 2^N]\!],\ p_{N,i} = p_0 - r_0 \sum_{j=1}^{2^N} q_j \left(1 + \sum_{(k,l) \in \Pi_{0 \to (N,i)}(N - \nu_{i-1,j-1})} \frac{1}{\xi_{k,l}}\right)$$

□

Remark 1.6. $A_N(\boldsymbol{\xi})$ is a real symmetric matrix and thus, can be diagonalized over $\mathbb{R}$ in an orthonormal basis of eigenvectors. There exist an orthogonal matrix $P \in \mathbb{R}^{2^N \times 2^N}$ and a diagonal matrix $D \in \mathbb{R}^{2^N \times 2^N}$ such that $A_N(\boldsymbol{\xi}) = P^\top D P$. P and D obviously depend on $\boldsymbol{\xi}$, but we decided it not to be mentioned for a sake of clarity.

Proposition 1.7. *The resistance matrix $A_N(\boldsymbol{\xi}) \in \mathbb{R}^{2^N \times 2^N}$ is invertible.*

Proof. By Remark 1.6, $A_N(\boldsymbol{\xi}) \in \mathbb{R}^{2^N \times 2^N}$ is a real symmetric matrix and thus, can be diagonalized over $\mathbb{R}$. Let $\lambda_{\min}$ be its smallest eigenvalue. We now use Courant-Fisher minimax theorem:

$$\lambda_{\min} = \min_{\substack{\boldsymbol{y} \in \mathbb{R}^{2^N \times 1} \\ \boldsymbol{y} \neq 0}} R(\boldsymbol{y}) \text{ with } R(\boldsymbol{y}) := \frac{\boldsymbol{y}^\top A_N(\boldsymbol{\xi}) \boldsymbol{y}}{\|\boldsymbol{y}\|^2}, \text{ the quotient of Rayleigh of } \mathbf{y}.$$

Let $\boldsymbol{y}$ be a nonzero vector in $\mathbb{R}^{2^N \times 1}$. It is well known (see for instance [21]) that

$$\boldsymbol{y}^\top A_N(\boldsymbol{\xi}) \boldsymbol{y} = r_0 \left(\frac{\left(\sum_{j=1}^{2^{N-1}} y_j\right)^2}{\xi_{1,1}} + \frac{\left(\sum_{j=2^{N-1}+1}^{2^N} y_j\right)^2}{\xi_{1,2}} + \cdots + \sum_{j=1}^{2^N} \frac{y_j^2}{\xi_{N,j}} + \sum_{j=1}^{2^N} y_j^2 \right). \tag{10}$$

Then, obviously, $\boldsymbol{y}^\top A_N(\boldsymbol{\xi}) \boldsymbol{y} \geq r_0 \|\boldsymbol{y}\|^2$. Thus, $R(\boldsymbol{y}) = \dfrac{\boldsymbol{y}^\top A_N(\boldsymbol{\xi}) \boldsymbol{y}}{\|\boldsymbol{y}\|^2} \geq r_0 > 0$. Therefore, by virtue of Courant-Fischer minimax theorem, $\lambda_{\min} > 0$ and, thus, all the eigenvalues of $A_N(\boldsymbol{\xi})$ are strictly positive which ends the proof. □

Example 1.8. So as to have an idea of the structure of the matrix $A_N(\boldsymbol{\xi})$, let us use an example of a tree with $N = 2$ levels (thus, with $N + 1 = 3$ generations, $2^{N-1} = 4$ outlets and $2^N - 1 = 7$ branches). Its resistance matrix $A_2(\boldsymbol{\xi}) \in \mathbb{R}^{4 \times 4}$ is defined as follows:

$$A_2(\boldsymbol{\xi}) := r_0 \begin{pmatrix} 1 + \frac{1}{\xi_{1,1}} + \frac{1}{\xi_{2,1}} & 1 + \frac{1}{\xi_{1,1}} & 1 & 1 \\ 1 + \frac{1}{\xi_{1,1}} & 1 + \frac{1}{\xi_{1,1}} + \frac{1}{\xi_{2,2}} & 1 & 1 \\ 1 & 1 & 1 + \frac{1}{\xi_{1,2}} + \frac{1}{\xi_{2,3}} & 1 + \frac{1}{\xi_{1,2}} \\ 1 & 1 & 1 + \frac{1}{\xi_{1,2}} & 1 + \frac{1}{\xi_{1,2}} + \frac{1}{\xi_{2,4}} \end{pmatrix}$$

The tree corresponding to this example is drawn on the figure 1.

From now, we assume fixed the pressures at the outlets of the tree and the flow in the tree root to Φ. Note that it implies that $\Phi = \sum_{j=1}^{2^N} q_{N,j}$.

Proposition 1.9. *The vector $\boldsymbol{q}$ is the unique solution of the linear system*

$$M_N(\boldsymbol{\xi}) \boldsymbol{q} = \boldsymbol{b_N} \tag{11}$$

where

$$M_N(\boldsymbol{\xi}) := \begin{pmatrix} (A_N(\boldsymbol{\xi}) \boldsymbol{v_1})^\top \\ \vdots \\ (A_N(\boldsymbol{\xi}) \boldsymbol{v_{2^N-1}})^\top \\ \boldsymbol{u_N}^\top \end{pmatrix} \in \mathbb{R}^{2^N \times 2^N}, \ \boldsymbol{b_N} := \begin{pmatrix} -\langle \boldsymbol{p}, \boldsymbol{v_1} \rangle \\ \vdots \\ -\langle \boldsymbol{p}, \boldsymbol{v_{2^N-1}} \rangle \\ \Phi \end{pmatrix} \in \mathbb{R}^{2^N \times 1} \tag{12}$$

and for all $i \in [\![1, 2^N - 1]\!]$, $\boldsymbol{v_i} := (0, \ldots, 0, 1, -1, 0, \ldots, 0)^\top \in \mathbb{R}^{2^N \times 1}$, with 1 at the i-th position and -1 at the $(i+1)$-th position.

Proof. The set of vectors $(\boldsymbol{v_i})_{i\in[1,2^N-1]}$ forms a basis of the orthogonal complement $\{\boldsymbol{u_N}\}^\perp$ of the vector $\boldsymbol{u_N}$. Let $i \in [\![1, 2^N - 1]\!]$. Multiplying (8) by $\boldsymbol{v_i}$ in the sense of the inner product yields

$$\forall i \in [\![1, 2^N - 1]\!] \, , \; -\langle \boldsymbol{p}, \boldsymbol{v_i}\rangle = \langle A_N(\boldsymbol{\xi})\boldsymbol{q}, \boldsymbol{v_i}\rangle. \tag{13}$$

Furthermore, by conservation of the flow rate, one has a relationship between the volumetric flow rate Φ which enters the tree and the flow rates $\boldsymbol{q}$ at the outlets of the tree $\langle \boldsymbol{q}, \boldsymbol{u_N}\rangle = \Phi$.

Thus, since $A_N(\boldsymbol{\xi})$ is real symmetric, the vector $\boldsymbol{q}$ verifies the following system

$$\begin{cases} \langle \boldsymbol{q}, A_N(\boldsymbol{\xi})\boldsymbol{v_i}\rangle = -\langle \boldsymbol{p}, \boldsymbol{v_i}\rangle, \; \forall i \in [\![1, 2^N - 1]\!] \\ \langle \boldsymbol{q}, \boldsymbol{u_N}\rangle = \Phi. \end{cases} \tag{14}$$

That explains the structure of the matrix $M_N(\boldsymbol{\xi})$. Let us now to prove that $M_N(\boldsymbol{\xi})$ is invertible. It amounts to proving that the set of vectors $(A_N(\boldsymbol{\xi})\boldsymbol{v_1}, \ldots, A_N(\boldsymbol{\xi})\boldsymbol{v_{2^N-1}}, \boldsymbol{u_N})$ is linearly independent. This is almost trivial that the set $(A_N(\boldsymbol{\xi})\boldsymbol{v_1}, \ldots, A_N(\boldsymbol{\xi})\boldsymbol{v_{2^N-1}})$ is linearly independent, combining the facts that $A_N(\boldsymbol{\xi})$ is invertible (by Proposition 1.7) and that the set $(\boldsymbol{v_i})_{i\in[1,2^N-1]}$ is obviously linearly independent.

Now, assume that

$$\lambda \boldsymbol{u_N} + \sum_{i=1}^{2^N-1} \mu_i A_N(\boldsymbol{\xi})\boldsymbol{v_i} = 0 \text{ with } (\lambda, \mu_1, \ldots, \mu_{2^N-1}) \in \mathbb{R}^{2^N}. \tag{15}$$

By Remark 1.6 and Proposition 1.7, $A_N(\boldsymbol{\xi}) = P^\top D P$ with $P \in \mathbb{R}^{2^N\times 2^N}$, $D = \operatorname{diag}\left(\{\lambda_i\}_{i\in[1,2^N]}\right)$, and all the eigenvalues of $A_N(\boldsymbol{\xi})$ are strictly positive. Hence, one has $A_N(\boldsymbol{\xi})^{-1} = \operatorname{diag}\left(\{\lambda_i^{-1}\}_{i\in[1,2^N]}\right)$ and it is possible to factorize $A_N(\boldsymbol{\xi})^{-1}$ as follows: $A_N(\boldsymbol{\xi})^{-1} = P^\top \delta^2 P$, where $\delta := \operatorname{diag}\left(\left\{\lambda_i^{-1/2}\right\}_{i\in[1,2^N]}\right)$.

Multiplying the equation (15) by the vector $A_N(\boldsymbol{\xi})^{-1}\boldsymbol{u_N}$ in the sense of the inner product yields

$$\lambda\langle \boldsymbol{u_N}, A_N(\boldsymbol{\xi})^{-1}\boldsymbol{u_N}\rangle + \sum_{i=1}^{2^N-1} \mu_i \langle A_N(\boldsymbol{\xi})\boldsymbol{v_i}, A_N(\boldsymbol{\xi})^{-1}\boldsymbol{u_N}\rangle = 0. \tag{16}$$

Since $\boldsymbol{v_i} \in \{\boldsymbol{u_N}\}^\perp$ for all $i \in [\![1, 2^N - 1]\!]$, it follows that

$$\langle A_N(\boldsymbol{\xi})\boldsymbol{v_i}, A_N(\boldsymbol{\xi})^{-1}\boldsymbol{u_N}\rangle = \langle \boldsymbol{v_i}, \boldsymbol{u_N}\rangle = 0, \; \forall i \in [\![1, 2^N - 1]\!] \, .$$

Moreover, $\langle \boldsymbol{u_N}, A_N(\boldsymbol{\xi})^{-1}\boldsymbol{u_N}\rangle = \|\delta P \boldsymbol{u_N}\|^2 > 0$, because $\boldsymbol{u_N} \neq 0$, $\det(P) \neq 0$ and $\det(\delta) \neq 0$.

The relation (16) yields $\lambda\|\delta P \boldsymbol{u_N}\|^2 = 0$. Hence, $\lambda = 0$ so that, by (15),

$$\sum_{i=1}^{2^N-1} \mu_i A_N(\boldsymbol{\xi})\boldsymbol{v_i} = 0.$$

By the linear independence of the set $(A_N(\boldsymbol{\xi})\boldsymbol{v_i})_{i\in[1,2^N-1]}$, we conclude that $\forall i \in [\![1, 2^N - 1]\!]$, $\mu_i = 0$.

Consequently, the set of vectors $(A_N(\boldsymbol{\xi})\boldsymbol{v_1}, \ldots, A_N(\boldsymbol{\xi})\boldsymbol{v_{2^N-1}}, \boldsymbol{u_N})$ is linearly independent. Thus, the matrix $M_N(\boldsymbol{\xi})$ is invertible, which ends the proof. □

1.2. **The optimization problems**

In this section, we will study a finite-dimensional constrained optimization problem. We use the notations introduced in the previous subsection 1.1. We consider the same rigid dyadic tree with $N + 1$ generations ($N \in \mathbb{N}, \; N \geq 1$) through which flows the same fluid as previously introduced. The tree is characterized by its

geometry $\boldsymbol{\xi}$ ($\boldsymbol{\xi} \in (\mathbb{R}_+^*)^{(2^{N+1}-2)\times 1}$), its resistance matrix $A_N(\boldsymbol{\xi})$ ($A_N(\boldsymbol{\xi}) \in \mathbb{R}^{2^N \times 2^N}$) and their volumetric flow rates $\boldsymbol{q}$ ($\boldsymbol{q} \in \mathbb{R}^{2^N \times 1}$) at the outlets of the tree.

We try to minimize the total viscous dissipated energy with respect to the variables $\boldsymbol{q}$ and $\boldsymbol{\xi}$ under constraints of Poiseuille-like flow and of constant volume.

It is well known (see [12, 21]) that the total viscous dissipated energy by the fluid during one second in the tree is, up to a multiplicative constant,

$$\mathcal{E}(\boldsymbol{q}, \boldsymbol{\xi}) := \boldsymbol{q}^\top A_N(\boldsymbol{\xi}) \boldsymbol{q}. \tag{17}$$

Since the tree is dyadic, it is usual to compute approximately the total volume V of the tree by summing the volume of each cylindrical branch, *i.e.*

$$\begin{aligned} V &= \pi R_0^2 L_0 + \sum_{(i,j)\in\mathcal{B}_N} \pi R_{i,j}^2 L_{i,j} = \pi R_0^2 L_0 \left(1 + \sum_{(i,j)\in\mathcal{B}_N} \left(\frac{R_{i,j}}{R_0}\right)^2 \frac{L_{i,j}}{L_0}\right) \\ &= \pi R_0^2 L_0 \left(1 + \sum_{(i,j)\in\mathcal{B}_N} \left(\frac{R_{i,j}}{R_0}\right)^3\right) = \pi R_0^2 L_0 \left(1 + \sum_{(i,j)\in\mathcal{B}_N} \prod_{(k,l)\in\Pi_{0\to(i,j)}} x_{k,l}\right) \\ &= \pi R_0^2 L_0 \left(1 + \sum_{(i,j)\in\mathcal{B}_N} \xi_{i,j}\right). \end{aligned} \tag{18}$$

Then, the constraint of total volume V comes down to

$$\sum_{(i,j)\in\mathcal{B}_N} \xi_{i,j} = \Lambda - 1 \tag{19}$$

where $\Lambda := \frac{V}{\pi R_0^2 L_0} > 1$, which is directly proportional to the total volume of the tree V.

From now on, we will not distinguish Λ and the total volume of the tree V.

One imposes another constraint on the geometry: lengths and radii of the tree are assumed to decrease as we go along its levels. More precisely,

$$\forall (i,j) \in \bigcup_{i\in[\![1,N-1]\!]} \mathcal{B}_{N,i},\ \max(\xi_{i+1,2j-1}, \xi_{i+1,2j}) \le \xi_{i,j}. \tag{20}$$

Finally, we define the set $\mathscr{A}_\Lambda$ by

$$\mathscr{A}_\Lambda := \left\{ \boldsymbol{\xi} \in (\mathbb{R}_+^*)^{(2^{N+1}-2)\times 1} \mid \boldsymbol{\xi} \text{ verifies the conditions (19) and (20)} \right\}. \tag{21}$$

1.2.1. *Case where the flow rate at the inlet and the pressures at the outlets are known*

The volumetric flow rate $\Phi > 0$ which enters the overall tree through the root branch and the pressures at the outlet of the tree (*i.e.* the vector $\boldsymbol{p}$, $\boldsymbol{p} \in (\mathbb{R}_+^*)^{2^N \times 1}$) are assumed to be fixed.

Let us define an admissible set $\mathscr{U}_\Lambda$ for the variables $(\boldsymbol{q}, \boldsymbol{\xi})$ as

$$\mathscr{U}_\Lambda := \left\{ (\boldsymbol{q}, \boldsymbol{\xi}) \mid \boldsymbol{\xi} \in \mathscr{A}_\Lambda \text{ and } \boldsymbol{q} = (M_N(\boldsymbol{\xi}))^{-1} \boldsymbol{b_N} \right\}. \tag{22}$$

Remark 1.10. This constraint comes down to impose an incompressible and Poiseuille-like flow through the tree (see Proposition 1.9).

Then, our optimization problem can be stated

$$(\mathscr{P})\begin{cases}\min \mathcal{E}(\boldsymbol{q},\boldsymbol{\xi})\\ (\boldsymbol{q},\boldsymbol{\xi})\in\mathscr{U}_\Lambda.\end{cases} \tag{23}$$

Let us set out the highlights of this section. First, we investigate the case where $(\mathscr{P})$ has a solution.

Theorem 1.11. *The problem $(\mathscr{P})$ has a solution if, and only if*

$$\boldsymbol{p}\in \mathrm{Span}(\boldsymbol{u_N}).$$

That is the case when all the pressures are equal at the outlets. Moreover,

$$\min_{(\boldsymbol{q},\boldsymbol{\xi})\in\mathscr{U}_\Lambda}\mathcal{E}(\boldsymbol{q},\boldsymbol{\xi})=r_0\Phi^2\left(1+\frac{N^2}{\Lambda-1}\right).$$

This theorem emphasizes the fact that if two pressures at the outlets are different, then, the problem $(\mathscr{P})$ has no solution. Nevertheless, we are able to exhibit a minimizing sequence. It has to be noticed that the value of the minimum does not differ according to the case considered.

Theorem 1.12. *Let us consider a dyadic tree whose number of generations is fixed, equal to $N+1$ ($N\in\mathbb{N}$, $N\geq 1$) and whose total volume is $\Lambda>1$. The volumetric flow rate $\Phi>0$ which enters the overall tree through the root branch and the pressures at the outlet of the tree are assumed to be fixed. Moreover, at least two pressures at the outlet are assumed to be different, which writes*

$$\exists j\in[\![1,2^N]\!]\mid p_{N,j}\neq p_{N,j+1}.$$

Then,

1. *the problem $(\mathscr{P})$ has no solution,*
2. *a minimizing sequence $(\boldsymbol{\xi}^\varepsilon,\boldsymbol{q}^\varepsilon)_{\varepsilon>0}$ is given by*

$$\begin{cases}\xi^\varepsilon_{i,j}:=\frac{\Lambda-1}{N}-\left(\frac{2^{N+1}-2}{N}-1\right)\varepsilon & \forall(i,j)\in\Pi_{0\to(N,1)},\\ \xi^\varepsilon_{i,j}:=\varepsilon & \forall(i,j)\in\mathcal{B}_N\backslash\Pi_{0\to(N,1)},\\ \boldsymbol{q}^\varepsilon=M_N(\boldsymbol{\xi}^\varepsilon)^{-1}\boldsymbol{b_N},\end{cases} \tag{24}$$

   with $\varepsilon>0$ sufficiently small to respect the constraint: $\forall(i,j)\in\mathcal{B}_N,\ \xi^\varepsilon_{i,j}>0$,

3. *One has*

$$m:=\inf_{(\boldsymbol{q},\boldsymbol{\xi})\in\mathscr{U}_\Lambda}\mathcal{E}(\boldsymbol{q},\boldsymbol{\xi})=r_0\Phi^2\left(1+\frac{N^2}{\Lambda-1}\right).$$

Remark 1.13. The sequence $(\boldsymbol{q}^\varepsilon)_{\varepsilon>0}$ converges to the vector $(\Phi,0,\dots,0)^\top$ when ε converges to zero. It boils down to the case in which the fluid exits the tree only by the outlet denoted by $(N,1)$. The use of some symmetry properties in the structure of the objective function $\mathcal{E}$ yields that we would easily get another minimizer by choosing any other outlet as main exit of the fluid, which would correspond to the closure of every path linking the root branch to the outlet except $\Pi_{0\to(N,i)}$, for any $i\in[\![1,2^N]\!]$. Note that the symmetry property does not hold for the pressures at outlets. However, when we take the limit in the minimizing sequence, since the flow is imposed, the pressure drop between the root and the outlet that remains open is the same whatever the outlet chosen. Thus, the pressure at root will depend on the pressure imposed at the outlet. This is the reason why it is well adapted to introduce the matrix $M_N(\boldsymbol{\xi})$, independent on the root pressure.

With a view to proving this theorem, one will proceed in two steps

1. firstly, determination of a lower bound for the total viscous dissipated energy,
2. secondly, construction of the minimizing sequence $(\boldsymbol{q}^\varepsilon,\boldsymbol{\xi}^\varepsilon)_{\varepsilon>0}$.

1.2.2. *Determination of a lower bound for the total viscous dissipated energy*

Let us now focus on an auxiliary optimization problem whose results turn out to be useful in the proof of Theorem 1.12. Let $\boldsymbol{q} \in \mathbb{R}^{(2^{N+1}-2)\times 1}$ and $\boldsymbol{\xi} \in (\mathbb{R}_+^*)^{(2^{N+1}-2)\times 1}$ be the two vectors

$$\boldsymbol{q} := (q_{1,1}, q_{1,2}, \dots, q_{N,1}, \dots, q_{N,2^N})^\top \text{ and } \boldsymbol{\xi} := (\xi_{1,1}, \xi_{1,2}, \dots, \xi_{N,1}, \dots, \xi_{N,2^N})^\top.$$

Notice that, in the rest of the paper and apart from the section 1.2.2, the notation $\boldsymbol{q}$ points out the vector only composed of the flow rates at the outlet of the tree.

Let $r_0 > 0$, $\Phi > 0$ and $\Lambda > 1$. Let $(\mathscr{Q})$ be the finite-dimensional constrained optimization problem

$$(\mathscr{Q}) \left\{ \begin{array}{l} \min \mathcal{E}(\boldsymbol{q}, \boldsymbol{\xi}) \\ \boldsymbol{q} \in \mathbb{R}^{(2^{N+1}-2)\times 1} \mid \forall i \in [\![1, N]\!], \ \displaystyle\sum_{j=1}^{2^i} q_{i,j} = \Phi \\ \boldsymbol{\xi} \in (\mathbb{R}_+^*)^{(2^{N+1}-2)\times 1} \mid \displaystyle\sum_{(k,l)\in\mathcal{B}_N} \xi_{k,l} = \Lambda - 1 \end{array} \right. \tag{25}$$

where $\mathcal{E}(\boldsymbol{q}, \boldsymbol{\xi})$ is defined by

$$\mathcal{E}(\boldsymbol{q}, \boldsymbol{\xi}) := r_0 \Phi^2 + \sum_{(k,l)\in\mathcal{B}_N} r_0 \frac{q_{k,l}^2}{\xi_{k,l}}. \tag{26}$$

Remark 1.14. It is sufficient to solve the problem $(\mathscr{Q})$ considering that the flow rates at the outlet are positive, *i.e.* $\boldsymbol{q} \in (\mathbb{R}_+)^{(2^{N+1}-2)\times 1}$. Indeed, since this energy is only composed of square terms, one has $\forall q_{1,1} \in \mathbb{R}$, $\mathcal{E}(-q_{1,1}, \dots) = \mathcal{E}(q_{1,1}, \dots)$ and so on for the other volumetric flow rates at the outlet of the tree.

Therefore, we will again denote by $(\mathscr{Q})$ the problem

$$(\mathscr{Q}) \left\{ \begin{array}{l} \min \mathcal{E}(\boldsymbol{q}, \boldsymbol{\xi}) \\ (\boldsymbol{q}, \boldsymbol{\xi}) \in \mathscr{C}_1 \times \mathscr{C}_2, \end{array} \right. \tag{27}$$

where

$$\begin{array}{rcl} \mathscr{C}_1 & = & \left\{ \boldsymbol{q} \in (\mathbb{R}_+)^{(2^{N+1}-2)\times 1} \mid \forall i \in [\![1, N]\!], \ \displaystyle\sum_{j=1}^{2^i} q_{i,j} = \Phi \right\} \\ \text{and } \mathscr{C}_2 & = & \left\{ \boldsymbol{\xi} \in (\mathbb{R}_+^*)^{(2^{N+1}-2)\times 1} \mid \displaystyle\sum_{(k,l)\in\mathcal{B}_N} \xi_{k,l} = \Lambda - 1 \right\}. \end{array}$$

Proposition 1.15. *The problem $(\mathscr{Q})$ has a solution $(\boldsymbol{q}^*, \boldsymbol{\xi}^*)$ and one has necessarily*

$$\forall (i,j) \in \mathcal{B}_N, \ q_{i,j}^* = \frac{N\Phi}{\Lambda - 1} \xi_{i,j}^*. \tag{28}$$

Moreover, the value of the minimum is equal to $r_0\Phi^2 \left(1 + \frac{N^2}{\Lambda - 1}\right)$.

Proof. One obviously has

$$\forall (\boldsymbol{q}, \boldsymbol{\xi}) \in \mathscr{C}_\Lambda, \ \mathcal{E}(\boldsymbol{q}, \boldsymbol{\xi}) \geq 0.$$

Therefore, the lower bound $\inf_{(\boldsymbol{q},\boldsymbol{\xi})\in\mathscr{C}_1\times\mathscr{C}_2} \mathcal{E}(\boldsymbol{q}, \boldsymbol{\xi})$ exists and is positive.

Since the constraints are uncoupled, it follows that

$$\inf_{(\boldsymbol{q},\boldsymbol{\xi})\in\mathscr{C}_1\times\mathscr{C}_2}\mathcal{E}(\boldsymbol{q},\boldsymbol{\xi})=\inf_{\boldsymbol{\xi}\in\mathscr{C}_2}\inf_{\boldsymbol{q}\in\mathscr{C}_1}\mathcal{E}(\boldsymbol{q},\boldsymbol{\xi}). \tag{29}$$

Let us first focus on the optimization problem, where $\boldsymbol{\xi}\in\mathscr{C}_2$ is fixed

$$(\mathscr{Q}_{\boldsymbol{\xi}})\begin{cases}\min\mathcal{E}(\boldsymbol{q},\boldsymbol{\xi})\\ \boldsymbol{q}\in\mathscr{C}_1\end{cases} \tag{30}$$

Any $\boldsymbol{q}\in\mathscr{C}_1$ verifies $\sum_{(i,j)\in\mathcal{B}_N}q_{i,j}=\sum_{(i,j)\in\mathcal{B}_N}|q_{i,j}|=N\Phi$. Therefore, $\mathscr{C}_1$ is closed and bounded. Since the energy $\mathcal{E}(.,\boldsymbol{\xi})$ is continuous as a polynomial function and strictly convex, on the convex compact set $\mathscr{C}_1$, then the problem $(\mathscr{Q}_{\boldsymbol{\xi}})$ has a unique solution.

By virtue of Kuhn-Tucker's theorem, there exists a real Lagrange multiplier μ_1 such that

$$\frac{\partial\mathcal{E}}{\partial q_{1,1}}=\frac{2r_0q_{1,1}}{\xi_{1,1}}=\mu_1\text{ and }\frac{\partial\mathcal{E}}{\partial q_{1,2}}=\frac{2r_0q_{1,2}}{\xi_{1,2}}=\mu_1. \tag{31}$$

Since $q_{1,1}+q_{1,2}=\Phi$, one has

$$q_{1,1}=\frac{r_0\xi_{1,1}}{\xi_{1,1}+\xi_{1,2}}\Phi\text{ and }q_{1,2}=\frac{r_0\xi_{1,2}}{\xi_{1,1}+\xi_{1,2}}\Phi. \tag{32}$$

Similarly,

$$\forall i\in[1,N],\ \forall j\in[\![1,2^i]\!],\ q_{i,j}=\frac{r_0\xi_{i,j}}{\sum_{k=1}^{2^i}\xi_{i,k}}\Phi. \tag{33}$$

Let us now focus on minimizing the functional $\boldsymbol{\xi}\in\mathscr{C}_2\mapsto\mathcal{E}(\boldsymbol{q}(\boldsymbol{\xi}),\boldsymbol{\xi})$. By (32) and (33), one has

$$\mathcal{E}(\boldsymbol{q}(\boldsymbol{\xi}),\boldsymbol{\xi})=r_0\Phi^2\left(1+\frac{1}{\xi_{1,1}+\xi_{1,2}}+\cdots+\frac{1}{\sum_{i=1}^{2^N}\xi_{N,i}}\right). \tag{34}$$

Let us use the change of variables

$$y_i:=\sum_{j=1}^{2^i}\xi_{i,j},\ i\in[\![1,2^N]\!]. \tag{35}$$

Then, our optimization problem becomes

$$\begin{cases}\min\left[r_0\Phi^2\left(1+\sum_{i=1}^{N}\frac{1}{y_i}\right)\right]\\ \sum_{i=1}^{N}y_i=\Lambda-1.\end{cases} \tag{36}$$

Thanks to Kuhn-Tucker's theorem, this minimum is obviously reached for $\boldsymbol{y}^*=(\frac{\Lambda-1}{N},\ldots,\frac{\Lambda-1}{N})$ and is equal to $r_0\Phi^2\left(1+\frac{N^2}{\Lambda-1}\right)$.

Consequently, the minimum of $\mathcal{E}$ over $\mathscr{C}_1\times\mathscr{C}_2$ is $r_0\Phi^2\left(1+\frac{N^2}{\Lambda-1}\right)$. Combining of (33) with the expression of $\boldsymbol{y}^*$ shows that, if $(\boldsymbol{q}^*,\boldsymbol{\xi}^*)$ denotes a minimizer of the optimization problem $(\mathscr{Q})$, one has necessarily

$$\forall(i,j)\in\mathcal{B}_N,\ q^*_{i,j}=\frac{N\Phi}{\Lambda-1}\xi^*_{i,j}. \tag{37}$$

□

Remark 1.16. The expression of the necessarily first-order optimality conditions in the proof of Proposition 1.15 leads easily to conclude that the problem $(\mathscr{Q})$ has an infinite number of minimizers.

Moreover, an interesting minimizing sequence $(\boldsymbol{q}^\varepsilon, \boldsymbol{\xi}^\varepsilon)_{\varepsilon>0}$ in $\mathscr{C}_1 \times \mathscr{C}_2$, of $\mathcal{E}$ for our problem is given by

$$\forall \varepsilon > 0, \begin{cases} \forall (i,j) \in \Pi_{0\to(N,1)}, & q^\varepsilon_{i,j} := \Phi \text{ and } \xi^\varepsilon_{i,j} := \frac{\Lambda-1}{N} - \left(\frac{2^{N+1}-2}{N} - 1\right)\varepsilon \\ \forall (i,j) \in \mathcal{B}_N \backslash \Pi_{0\to(N,1)}, & q^\varepsilon_{i,j} := 0 \text{ and } \xi^\varepsilon_{i,j} := \varepsilon. \end{cases} \tag{38}$$

Physically, this is the case where the fluid exits the tree only by the outlet denoted by $(N, 1)$.

1.2.3. *Proof of the theorem 1.11*

Since the problem $(\mathscr{Q})$ is less constrained than $(\mathscr{P})$, the solution of $(\mathscr{P})$ needs to respect the necessary first-order optimality conditions for the problem $(\mathscr{Q})$, namely

$$\forall (i,j) \in \mathcal{B}_N,\ q_{i,j} = \frac{N\xi_{i,j}}{\Lambda - 1}\Phi. \tag{39}$$

Let us denote as previously by p_0 the pressure at the inlet of the tree. According to the Poiseuille law and reasoning by induction, one has

$$\left\{ \begin{array}{l} \left.\begin{array}{l} p_0 - p_{1,1} = \frac{N\Phi}{\Lambda-1} \\ p_0 - p_{1,2} = \frac{N\Phi}{\Lambda-1} \end{array}\right\} \Longrightarrow p_{1,1} = p_{1,2} \\ \qquad \vdots \\ \left.\begin{array}{l} p_{i,j} - p_{i+1,2j-1} = \frac{N\Phi}{\Lambda-1} \\ p_{i,j} - p_{i+1,2j} = \frac{N\Phi}{\Lambda-1} \end{array}\right\} \Longrightarrow p_{i+1,2j-1} = p_{i+1,2j}, \forall (i,j) \in \bigcup_{i\in[1,N-1]} \mathcal{B}_{N,i}. \end{array} \right.$$

In particular, it implies that

$$p_{N,1} = p_{N,2} = \cdots = p_{N,2^N-1} = p_{N,2^N}.$$

Reversely, let us prove that, if there exists $\overline{p} \in \mathbb{R}$ such that $\boldsymbol{p} = \overline{p}\boldsymbol{u_N}$, then, the problem $(\mathscr{P})$ has a solution. In this case, we are able to exhibit an element $(\boldsymbol{q}, \boldsymbol{\xi})$ which belongs to the admissible set $\mathscr{U}_\Lambda$. For instance, let us take

$$\forall (i,j) \in \mathcal{B}_N,\ \xi_{i,j} := \frac{\Lambda - 1}{N 2^i}.$$

Then, it is easy to make the calculation of the flow throughout the tree. Indeed

$$\left.\begin{array}{l} p_{N-1,1} - p_{N,1} = \frac{q_{N,1}}{\xi_{N,1}} \\ p_{N-1,1} - p_{N,2} = \frac{q_{N,2}}{\xi_{N,2}} \end{array}\right\} \Longrightarrow q_{N,1} = q_{N,2} \text{ since } p_{N,1} = p_{N,2} = \overline{p} \text{ and } \xi_{N,1} = \xi_{N,2}.$$

Iterating this reasoning proves that $\boldsymbol{q} \in \mathrm{Span}(\boldsymbol{u_N})$ and more generally, by induction, we obtain

$$\forall (i,j) \in \mathcal{B}_N,\ q_{i,j} = \frac{\Phi}{2^i}.$$

In other terms, the flows at the i-th level ($i \in [1, N]$) are the same. Then, we obtain that

$$\forall (i,j) \in \mathcal{B}_N,\ \frac{q_{i,j}}{\xi_{i,j}} = \frac{N\Phi}{\Lambda - 1}.$$

We find again the first order optimality condition for the problem $(\mathscr{Q})$. Let us remind that, by convexity arguments, the solution of the problem $(\mathscr{Q})$ is determined in a unique way by the first order optimality conditions. It ensures that the minimum is equal to m and that the problem $(\mathscr{P})$ has a solution in this case.

Moreover, notice that $\forall (i,j) \in \mathcal{B}_N$, with $i > 1$, $x_{i,j} = \frac{1}{2}$. It corresponds to the case where the ratio of two consecutive radii of the tree is equal to $\left(\frac{1}{2}\right)^{\frac{1}{3}}$ in the whole tree. It is the same solution as the optimization problem of symmetric trees studied in [20].

1.2.4. *Proof of the theorem 1.12*

Definition 1.17. U_N is the matrix of size $2^N \times 2^N$ whose coefficients are all equal to 1.

Let us consider the optimization problem $(\mathscr{P})$ for a given N.
Let the sequence $(\boldsymbol{\xi}^\varepsilon)_{\varepsilon>0}$ (for all $\varepsilon > 0$, $\boldsymbol{\xi}^\varepsilon \in (\mathbb{R}_+^*)^{6\times 1}$) be defined by

$$\begin{cases} \xi^\varepsilon_{1,1} = \xi^\varepsilon_{2,1} = \cdots = \xi^\varepsilon_{N,1} = \frac{\Lambda-1}{N} - \left(\frac{2^{N+1}-2}{N} - 1\right)\varepsilon \\ \xi^\varepsilon_{i,j} = \varepsilon, \ \ \forall (i,j) \in [1,N] \times [\![2, 2^i]\!] \, . \end{cases} \tag{40}$$

We define m by $m := \min\limits_{\mathscr{C}_\Lambda} \mathcal{E} = r_0 \Phi^2 \left(\dfrac{N^2}{\Lambda - 1} + 1\right)$. Let us show that $\lim\limits_{\varepsilon \to 0} \mathcal{E}(\boldsymbol{q}(\boldsymbol{\xi}^\varepsilon), \boldsymbol{\xi}^\varepsilon) = m$ where $\boldsymbol{q}(\boldsymbol{\xi}^\varepsilon)$ is the unique solution of the linear system $M_N(\boldsymbol{\xi}^\varepsilon)\boldsymbol{q} = \boldsymbol{b_N}$ (see Proposition 1.9). Let us denote $\boldsymbol{q}(\boldsymbol{\xi}^\varepsilon)$ by $\boldsymbol{q}^\varepsilon$, $A_N(\boldsymbol{\xi}^\varepsilon)$ by $A_N(\varepsilon)$ and $M_N(\boldsymbol{\xi}^\varepsilon)$ by $M_N(\varepsilon)$.

Let us recall that, according to Proposition 1.9, the vector $\boldsymbol{q}^\varepsilon$ is completely characterized by the system

$$\begin{cases} \langle \boldsymbol{q}^\varepsilon, A_N(\varepsilon)\boldsymbol{v_i}\rangle = -\langle \boldsymbol{p}, \boldsymbol{v_i}\rangle, \ \forall i \in [\![1, 2^N - 1]\!] \\ \langle \boldsymbol{q}^\varepsilon, \boldsymbol{u_N}\rangle = \Phi \end{cases} \tag{41}$$

with

$$\forall \varepsilon > 0, \ A_N(\varepsilon) = r_0 \left(U_N + \frac{1}{\varepsilon}\widetilde{A}_N + \frac{1}{\frac{\Lambda-1}{N} - \left(\frac{2^{N+1}-2}{N} - 1\right)\varepsilon}\widetilde{B}_N \right) \tag{42}$$

where U_N, $\widetilde{A}_N$ and $\widetilde{B}_N$ are three matrices independent of ε with same size as $A_N(\varepsilon)$.

The first one, U_N, comes from the root branch that adds a resistance r_0 to the resistance of any pathway in the tree. The second one, $\widetilde{A}_N$ is more precisely characterized in the lemma 1.19. $\widetilde{A}_N$, corresponds to the resistance matrix of the pathways consisting only in branches (i,j) such that $\xi_{i,j} = \varepsilon$ (i.e. whose diameter will go to 0 with ε), namely all pathways in the tree except those included in the pathway going from the root to the outlet $(N,1)$. These last pathways are finally accounted for in the third part B_N and corresponds to those that stay open when ε goes to 0.

Defining $\widetilde{A}_N(\varepsilon) := \varepsilon A_N(\varepsilon)$, we have

$$\lim_{\varepsilon \to 0} \widetilde{A}_N(\varepsilon) = r_0 \widetilde{A}_N \tag{43}$$

Therefore, the vector $\boldsymbol{q}^\varepsilon$ is completely characterized by the system

$$\begin{cases} \langle \boldsymbol{q}^\varepsilon, \widetilde{A}_N(\varepsilon)\boldsymbol{v_i}\rangle = -\varepsilon\langle \boldsymbol{p}, \boldsymbol{v_i}\rangle, \ \forall i \in [\![1, 2^N - 1]\!] \, , \\ \langle \boldsymbol{q}^\varepsilon, \boldsymbol{u_N}\rangle = \Phi \end{cases} \tag{44}$$

Thus it is necessary to study more closely the matrix $\widetilde{A}_N$ that will give the behavior of $\boldsymbol{q}^\varepsilon$ when ε goes to 0.

Definition 1.18. Let m and n be two nonzero integers. Let $A_1 \in \mathbb{R}^{n\times n}$ and $A_2 \in \mathbb{R}^{m\times m}$ be two matrices. We define the direct sum of A_1 and A_2 as the matrix M in $\mathbb{R}^{n+m,n+m}$ defined by blocks:

$$M = A_1 \oplus A_2 := \left(\begin{array}{c|c} A_1 & 0 \\ \hline 0 & A_2 \end{array}\right).$$

We have the following property:

Lemma 1.19. *$\widetilde{A}_N = (0) \oplus \bigoplus_{p=0}^{N-2} B_p$ where B_p is a resistance matrix of a tree of $p+1$ generations whose branches have all the same resistance equal to 1.*

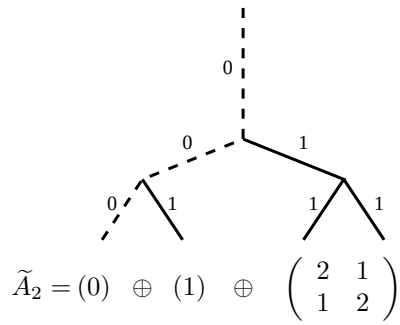

$$\widetilde{A}_2 = \begin{pmatrix} 0 & 0 & 0 & 0 \\ 0 & 1 & 0 & 0 \\ 0 & 0 & 2 & 1 \\ 0 & 0 & 1 & 2 \end{pmatrix}$$

FIGURE 2. Example of the matrix $\widetilde{A}_N$ for $N = 2$. The numbers next to the branches represent their resistance. The matrix $\widetilde{A}_N$ is the direct sum of the resistance matrices of the subtrees built up by branches with non zero resistance.

Proof. From its definition, $\widetilde{A}_N$ corresponds to the resistance matrix of a tree with $N+1$ generations where the resistances of the branches on the path from root to outlet $(N, 1)$ are all 0 and the resistance of the other branches are all 1. □

Now, system (44) is equivalent to

$$\widetilde{M}_N(\varepsilon)\boldsymbol{q}^\varepsilon = \widetilde{\boldsymbol{b}}_{\boldsymbol{N}}(\varepsilon) \tag{45}$$

where

$$\widetilde{M}_N(\varepsilon) := \begin{pmatrix} (\widetilde{A}_N(\varepsilon)\boldsymbol{v_1})^\top \\ \vdots \\ (\widetilde{A}_N(\varepsilon)\boldsymbol{v_{2^N-1}})^\top \\ \boldsymbol{u_N}^\top \end{pmatrix} \text{ and } \widetilde{\boldsymbol{b}}_{\boldsymbol{N}}(\varepsilon) := \begin{pmatrix} -\varepsilon\langle \boldsymbol{p}, \boldsymbol{v_1}\rangle \\ \vdots \\ -\varepsilon\langle \boldsymbol{p}, \boldsymbol{v_{2^N-1}}\rangle \\ \Phi \end{pmatrix} \tag{46}$$

(47)

One has

$$\lim_{\varepsilon\to 0} \widetilde{M}_N(\varepsilon) = \widetilde{M}_N \text{ and } \lim_{\varepsilon\to 0} \widetilde{\boldsymbol{b}}_{\boldsymbol{N}}(\varepsilon) = \widetilde{\boldsymbol{b}}_{\boldsymbol{N}} \tag{48}$$

where

$$\widetilde{M}_N := \begin{pmatrix} r_0(\widetilde{A}_N\boldsymbol{v_1})^\top \\ \vdots \\ r_0(\widetilde{A}_N\boldsymbol{v_{2^N-1}})^\top \\ \boldsymbol{u_N}^\top \end{pmatrix} \quad \text{and} \quad \widetilde{\boldsymbol{b}}_{\boldsymbol{N}} := \begin{pmatrix} 0 \\ \vdots \\ 0 \\ \Phi \end{pmatrix} \tag{49}$$

Proposition 1.20. *The matrix $\widetilde{M}_N$ is invertible.*

Proof. We will show that the family $\left((\widetilde{A}_N\boldsymbol{v_i})_{i=1\dots 2^N-1}, \boldsymbol{u_N}\right)$ is independant. Let $(\lambda_i)_{i=1\dots 2^N-1}$ and μ be real numbers such that

$$\mu\boldsymbol{u_N} + \sum_{i=1}^{2^N-1} \lambda_i \widetilde{A}_N\boldsymbol{v_i} = 0 \tag{50}$$

Let us recall from lemma 1.19 that $\widetilde{A}_N = (0) \oplus \bigoplus_{p=0}^{N-2} B_p$ with B_p's resistance matrix and thus invertible.

Consequently, $\mathrm{Rg}(\widetilde{A}_N) = \mathrm{Span}\,(\boldsymbol{e_2}, \ldots, \boldsymbol{e_{2^N}})$. This implies that, in equation (50) the composant along $\boldsymbol{e_1}$ is reduced to $\mu = 0$.

Now, the restriction of $\widetilde{A}_N$ on its image is a bijection, therefore as soon as the projection of the family $(\boldsymbol{v_i})_{i=1\ldots 2^N-1}$ on $\mathrm{Rg}(\widetilde{A}_N) = \mathrm{Span}\,(\boldsymbol{e_2}, \ldots, \boldsymbol{e_{2^N}})$ is a base of $\mathrm{Rg}(\widetilde{A}_N)$, which is true in our case, then the family $(\widetilde{A}_N \boldsymbol{v_i})_{i=1\ldots 2^N-1}$ is independant and all λ_i's are 0. □

Using the continuity of the map $A \longmapsto A^{-1}$ where A is an invertible matrix, the unique solution of $\widetilde{M}_N(\varepsilon)\boldsymbol{q}^\varepsilon = \widetilde{\boldsymbol{b}}_{\boldsymbol{N}}$ converges to the unique solution of the system $\widetilde{M}_N \left(\lim_{\varepsilon\to 0} \boldsymbol{q}^\varepsilon\right) = \widetilde{\boldsymbol{b}}_{\boldsymbol{N}}$. Moreover, we know that $\widetilde{M}_N \boldsymbol{e_1} = (r_0 \boldsymbol{v_1}^\top \widetilde{A}_N^\top \boldsymbol{e_1}, \ldots, r_0 \boldsymbol{v_{2^N-1}}^\top \widetilde{A}_N^\top \boldsymbol{e_1}, \boldsymbol{u_N}^\top \boldsymbol{e_1}) = \boldsymbol{e_{2^N}}$ because $\widetilde{A}_N^\top = \widetilde{A}_N$ and $\mathrm{Ker}(\widetilde{A}_N) = \mathrm{Span}\,(\boldsymbol{e_1})$. Finally,

$$\lim_{\varepsilon\to 0} \boldsymbol{q}^\varepsilon = \widetilde{M}_N^{-1} \widetilde{\boldsymbol{b}}_{\boldsymbol{N}} = \Phi \widetilde{M}_N^{-1} \boldsymbol{e_{2^N}} = \Phi \boldsymbol{e_1}. \tag{51}$$

Remark 1.21. One should notice that all the elements of the sequence $(\boldsymbol{q}^\varepsilon, \boldsymbol{\xi}^\varepsilon)_{\varepsilon>0}$ are in $\mathscr{U}_\Lambda$ but not its limit.

Then, since we have $\widetilde{\boldsymbol{b}}_{\boldsymbol{N}} = \varepsilon\boldsymbol{\gamma} + \Phi \boldsymbol{e_{2^N}}$, with $\boldsymbol{\gamma} \in \mathrm{Span}\,(e_1, \ldots, e_{2^N-1})$, we have $\boldsymbol{q}^\varepsilon = \widetilde{M}_N(\varepsilon)^{-1} \widetilde{\boldsymbol{b}}_{\boldsymbol{N}} = \varepsilon \widetilde{M}_N(\varepsilon)^{-1}\gamma + \Phi \boldsymbol{e_1}$ and

$$\begin{aligned}
\mathcal{E}(\boldsymbol{q}^\varepsilon, \boldsymbol{\xi}^\varepsilon) &:= (\boldsymbol{q}^\varepsilon)^\top A_N(\boldsymbol{\xi}^\varepsilon) \boldsymbol{q}^\varepsilon \\
&= \left(\varepsilon \boldsymbol{\gamma}^\top \left(\widetilde{M}_N(\varepsilon)^{-1}\right)^\top + \Phi \boldsymbol{e_1}^\top\right) A_N(\varepsilon) \left(\varepsilon \widetilde{M}_N(\varepsilon)^{-1} \boldsymbol{\gamma} + \Phi \boldsymbol{e_1}\right) \\
&= \varepsilon^2 \boldsymbol{\gamma}^\top \left(\widetilde{M}_N(\varepsilon)^{-1}\right)^\top A_N(\varepsilon) \widetilde{M}_N(\varepsilon)^{-1} \boldsymbol{\gamma} \\
&\quad + \varepsilon\Phi \boldsymbol{\gamma}^\top \left(\widetilde{M}_N(\varepsilon)^{-1}\right)^\top A_N(\varepsilon) \boldsymbol{e_1} \\
&\quad + \varepsilon\Phi \boldsymbol{e_1}^\top A_N(\varepsilon) \widetilde{M}_N(\varepsilon)^{-1} \boldsymbol{\gamma} \\
&\quad + \Phi^2 \boldsymbol{e_1}^\top A_N(\varepsilon) \boldsymbol{e_1}
\end{aligned}$$

Since $\lim_{\varepsilon\to 0} (\varepsilon A_N(\varepsilon)) = \widetilde{A}_N$ and $\lim_{\varepsilon\to 0} \widetilde{M}_N(\varepsilon) = \widetilde{M}_N$, then one successively has

$$\begin{aligned}
\varepsilon^2 \boldsymbol{\gamma}^\top \left(\widetilde{M}_N(\varepsilon)^{-1}\right)^\top A_N(\varepsilon) \widetilde{M}_N(\varepsilon)^{-1} \boldsymbol{\gamma} &\xrightarrow[\varepsilon\to 0]{} 0 \\
\varepsilon\Phi \boldsymbol{\gamma}^\top \left(\widetilde{M_N}(\varepsilon)^{-1}\right)^\top A_N(\varepsilon) \boldsymbol{e_1} &\xrightarrow[\varepsilon\to 0]{} 0 \\
\varepsilon\Phi \boldsymbol{e_1}^\top A_N(\varepsilon) \widetilde{M}_N(\varepsilon)^{-1} \boldsymbol{\gamma} &\xrightarrow[\varepsilon\to 0]{} 0 \\
\Phi^2 \boldsymbol{e_1}^\top A_N(\varepsilon) \boldsymbol{e_1} &\xrightarrow[\varepsilon\to 0]{} \left(1 + \tfrac{N^2}{\Lambda-1}\right) r_0 \Phi^2,
\end{aligned} \tag{52}$$

because $\widetilde{A}_N \boldsymbol{e_1} = 0$, $\boldsymbol{e_1}^\top \widetilde{A}_N^\top = 0$ and $\boldsymbol{e_1}^\top A_N(\varepsilon) \boldsymbol{e_1} = r_0 + \frac{N r_0}{\frac{\Lambda-1}{N} - \left(\frac{2^{N+1}-2}{N} - 1\right)\varepsilon}$. Hence,

$$\lim_{\varepsilon\to 0} \mathcal{E}(\boldsymbol{q}^\varepsilon, \boldsymbol{\xi}^\varepsilon) = r_0 \Phi^2 \left(\frac{N^2}{\Lambda - 1} + 1\right) = m,$$

where m is the minimum of $\mathcal{E}$ over $\mathscr{C}_\Lambda$ (see Problem $(\mathscr{Q})$). Since $(\mathscr{Q})$ is less constrained than $(\mathscr{P})$, the sequence $(\boldsymbol{q}^\varepsilon, \boldsymbol{\xi}^\varepsilon)_{\varepsilon>0}$ is a minimizing sequence of $\mathcal{E}$ over $\mathscr{U}_\Lambda$ and m is the lower bound of $\mathcal{E}$ over $\mathscr{U}_\Lambda$.

1.2.5. *Case where the flow rates at the outlets are known*

This case is much simpler than the one presented in section 1.2.1. Using the same notations as in this section, we introduce a new optimization problem

$$(\mathscr{P}') \ \begin{cases} \min \mathcal{E}(\boldsymbol{q}, \boldsymbol{\xi}) \\ \boldsymbol{\xi} \in \mathscr{A}_\Lambda, \end{cases} \tag{53}$$

where the vector of the flow rates at the outlets of the tree, $\boldsymbol{q} \in \mathbb{R}_+^{2^N \times 1}$, is assumed to be fixed, and $\mathscr{A}_\Lambda$ is the set defined in the formula (21). It can be noticed that, under these assumptions, and since the volumetric flow rate is conserved along the tree, every value of the intermediate flow rate $q_{i,j}$ is known, from the values of $q_{N,j}$, $j \in [\![1, 2^N]\!]$.

In this case, the existence of a solution for this problem is obvious. Indeed, letting one of the optimization variables go to zero implies that the energy tends to a positive infinite value. It is thus possible to come down to minimize $\mathcal{E}(\boldsymbol{q}, \cdot)$ on a compact set, which gives the existence. Moreover, since $\mathscr{A}_\Lambda$ is a convex set and $\mathcal{E}(\boldsymbol{q}, \cdot)$ is obviously strictly convex, the minimizer is unique for that problem.

Let us now write the first order optimality conditions: we denote by $\boldsymbol{\xi}^*$ the minimizer of the problem $(\mathscr{P}')$. There exists a Lagrange multiplier $\lambda \in \mathbb{R}$ such that

$$\forall (i,j) \in \mathcal{B}_N, \ \frac{q_{i,j}}{\xi_{i,j}} = -\lambda.$$

Using the volume contraint, we immediately obtain the following expression for the minimizer $\boldsymbol{\xi}^*$:

$$\forall (i,j) \in \mathcal{B}_N, \ \xi^*_{i,j} = (\Lambda - 1) \frac{q_{i,j}^2}{\sum_{(i,j) \in \mathcal{B}_N} q_{i,j}^2}.$$

Unlike the case where the flow rate at the inlet and the pressures at the outlets are known, every branch of the tree remains open in this case.

2. Case of a fluid driven by Navier-Stokes equations: some numerical results

As announced in the title and the introduction of this paper, we are interested in this section in an infinite dimensional optimization problem. Indeed, we present an augmented-Lagrangian like algorithm and implement it to optimize the shape of dyadic trees crossed by a fluid driven by a Stokes or Navier-Stokes system. We focus here on the 3D case but the 2D case can be easily adapted from this 3D study.

The partial differential equation describing the behaviour of the fluid and the boundary conditions have been chosen for a sake of generality. In particular, this model is convenient to be used in the modelling of the bronchial tree. (see for instance [12, 17–20])

This section is organized as follows: in 2.1, we introduce the Navier-Stokes like fluid model, the notations, and recall some general results of Fluid Mechanics on the existence, uniqueness and smoothness of the velocity and pressure. In 2.2, we roughly present the shape optimization problem, give the expression of the derivative with respect to the domain thanks to the so called Hadamard's method (see [1, 13, 23, 25]). We also give a precise description of the augmented-Lagrangian method in shape optimization, present our algorithm and its implementation. In 2.3 are presented the numerical results obtained thanks to this method with the software *Comsol*.

2.1. **Optimization of a bifurcation**

Let us now precise the frame of our study. We begin by defining a notion of bifurcation for a domain Ω.

Definition 2.1. A domain Ω of $\mathbb{R}^3$ defines a bifurcation if

(1) Ω is simply connected.
(2) its boundary $\partial\Omega$ has a Lipschitz regularity ;
(3) $\partial\Omega$ contains three disks: an inlet E and two outlets whose union is denoted by S ;

For a given bifurcation Ω we define the lateral boundary $\Gamma := \partial\Omega\backslash(E \cup S)$.

In what follows, we assume that E is contained in the hyperplane $\{x_3 = 0\}$. Let us now precise the law driving the behaviour of the fluid we will impose.

Definition 2.2. Let $\boldsymbol{u}$ be a smooth vector field of $\mathbb{R}^3$ (for instance C^1). As usually in Fluid Mechanics, we define

(1) the stretching tensor of $\boldsymbol{u}$ (symmetric part of the gradient tensor):

$$\varepsilon(\boldsymbol{u}) := \left(\frac{1}{2}\left(\frac{\partial u_i}{\partial x_j} + \frac{\partial u_j}{\partial x_i}\right)\right)_{1\leq i,j\leq 3}.$$

(2) the doubly contracted product of two stretching tensors $\varepsilon(\boldsymbol{u})$ and $\varepsilon(\boldsymbol{v})$:

$$\varepsilon(\boldsymbol{u}) : \varepsilon(\boldsymbol{v}) := \frac{1}{4}\sum_{i=1}^{3}\sum_{j=1}^{3}\left(\frac{\partial u_i}{\partial x_j} + \frac{\partial u_j}{\partial x_i}\right)\left(\frac{\partial v_i}{\partial x_j} + \frac{\partial v_j}{\partial x_i}\right).$$

(3) the strain tensor of $(\boldsymbol{u}, p)$, where $\boldsymbol{u}$ is a smooth vector field of $\mathbb{R}^3$ representing the velocity of a fluid whose viscosity is $\mu > 0$ and p a function representing the pressure defined on $\mathbb{R}^3$:

$$\sigma(\boldsymbol{u}, p) := -pI_3 + 2\mu\varepsilon(\boldsymbol{u}),$$

where I_3 is the identity tensor of $\mathbb{R}^3$.

Let Ω be a bifurcation. We assume that Ω is crossed by a fluid driven by the Navier-Stokes laws. In particular, this model is convenient to represent to upper part of the bronchial tree since the velocity of the air at the beginning of the trachea is important enough to consider that the flow is turbulent. In this case, the regime of the fluid is turbulent.
Let us assume that Ω is crossed by a viscous incompressible newtonian fluid. A plausible model is given by a choice of the velocity $\boldsymbol{u} : \Omega \to \mathbb{R}^3$ and the pressure $p : \Omega \to \mathbb{R}$ as solutions of the Navier-Stokes system

$$\begin{cases} -\mu\Delta\boldsymbol{u} + \nabla p + \nabla\boldsymbol{u}\cdot\boldsymbol{u} = 0 & x \in \Omega \\ \nabla\cdot\boldsymbol{u} = 0 & x \in \Omega \\ \boldsymbol{u} = \boldsymbol{u_0} & x \in E \\ \boldsymbol{u} = 0 & x \in \Gamma \\ -p\boldsymbol{n} + 2\mu\varepsilon(\boldsymbol{u})\cdot\boldsymbol{n} = \boldsymbol{h} & x \in S, \end{cases} \tag{54}$$

where

- $\boldsymbol{n}$ denotes the outward-pointing unit normal vector at a given point of the boundary $\partial\Omega$,
- $\boldsymbol{u_0}$ is a parabolic velocity profile (*i.e.* a Poiseuille's flow is imposed at the inlet E), that is

$$\boldsymbol{u_0} = (0, 0, c(r^2 - R^2))^\top,$$

where c is a negative constant so that the flow is ingoing, and R the radius of the inlet.

Remark 2.3. Let us focus on the choice of the boundary conditions for this model.

- The condition $\boldsymbol{u} = 0$ on Γ is the so-called *no-slip* boundary condition and consists in assuming that the fluid does not slip on a solid surface.
- Practically speaking, we will impose $\boldsymbol{h} = -p_0\boldsymbol{n}$ at the outlet S. This condition comes down more or less in assuming that the pressure is known on S and equal to p_0. Drawing a comparison with the modelling of the bronchial tree, these conditions mimick muscles using the same energy to pump the air into the lung (see [12]). Similar boundary conditions are much studied in [5, chapter 5] and in [6, 7].

Notice that classical theory on Navier-Stokes equations (see [11, 26]) gives an existence and uniqueness result for system (54):

Theorem 2.4. *Let Ω be a bounded Lipschitz domain of $\mathbb{R}^3$. Let us assume that $\boldsymbol{u_0}$ belongs to the Sobolev space $(\mathrm{H}^{3/2}(E))^3$ and $\boldsymbol{h}$ belongs to $(\mathrm{H}^{1/2}(S))^3$. If the viscosity μ is large enough, then the problem (54) has a unique solution $(\boldsymbol{u}, p) \in (\mathrm{H}^1(\Omega))^3 \times \mathrm{L}^2(\Omega)$.*

Remark 2.5. Let us introduce the functional spaces

$$\begin{aligned} W_0(\Omega) &:= \left\{(\boldsymbol{v}, q) \in (\mathrm{H}^1(\Omega))^3 \times \mathrm{L}^2(\Omega) : \boldsymbol{v} = 0 \text{ on } E \cup \Gamma\right\}. \\ Z_{\boldsymbol{u_0}}(\Omega) &:= \left\{(\boldsymbol{v}, q) \in (\mathrm{H}^1(\Omega))^3 \times \mathrm{L}^2(\Omega) : \boldsymbol{v} = \boldsymbol{u}_0 \text{ on } E \text{ and } \boldsymbol{v} = 0 \text{ on } \Gamma\right\}. \end{aligned}$$

The variational formulation of the Navier-Stokes system (54) writes

$$\left\{ \begin{array}{l} \text{Find } (\boldsymbol{u}, p) \in Z_{\boldsymbol{u_0}}(\Omega) \text{ s.t. } \forall (\boldsymbol{w}, \psi) \in W_0(\Omega), \\ \displaystyle\int_\Omega (2\mu\varepsilon(\boldsymbol{u}) : \varepsilon(\boldsymbol{w}) + \nabla\boldsymbol{u}\cdot\boldsymbol{u}\cdot\boldsymbol{w} - p\nabla\cdot\boldsymbol{w})\,\mathrm{d}x = \int_S \boldsymbol{h}\cdot\boldsymbol{w}\mathrm{d}s \\ \displaystyle\int_\Omega \psi\nabla\cdot\boldsymbol{u}\mathrm{d}x = 0. \end{array} \right. \tag{55}$$

Let us now introduce the shape optimization problem we want to solve numerically. The objective functional $J(\Omega)$ is the energy dissipated by the fluid, *i.e.*

$$J(\Omega) := 2\mu \int_\Omega |\varepsilon(\boldsymbol{u})|^2 \mathrm{d}x \tag{56}$$

To make the statement of the optimization problem precise, we need to define the class of admissible shapes. As classically in shape optimization, we fix the measure $V_0 > 0$ of Ω:

$$\mathcal{O}_{V_0} := \left\{\Omega \text{ bounded and simply connected domain in } \mathbb{R}^3 \mid \mathrm{meas}(\Omega) = V_0,\ \Pi_E \cap \overline{\Omega} = E,\ (\Pi_S^1 \cup \Pi_S^2) \cap \overline{\Omega} = S\right\}, \tag{57}$$

where Π_E is the affine hyperplane spanned by E, Π_S^1 and Π_S^2 the two affine hyperplanes spanned by S. Thus the shape optimization problem writes

$$\left\{ \begin{array}{l} \min J(\Omega) \\ \Omega \in \mathcal{O}_{V_0}, \end{array} \right. \tag{58}$$

where V_0 is a positve given real number.

The question of knowing if the problem (58) has or not a solution is still an open problem. Nevertheless, it is possible to show that a problem, very close to the problem (58) but a little bit constrained, has a solution.

Restricting the set of admissible shapes is a very common approach in shape optimization, since these problems are often ill-posed (see for instance [1,13]). We present now an existence result by considering instead of the set $\mathcal{O}_{V_0}$, a set of domains verifying an ε-cone property, which yields some kind of uniform regularity. (see [8,9,13] for some reminders on the ε-cone property and its consequences on the existence of optimal shapes)

In that purpose, let us define for $\varepsilon > 0$ the class

$$\mathcal{O}_{V_0}^{\varepsilon} := \{\Omega \in \mathcal{O}_{V_0} \mid \Omega \text{ has the } \varepsilon\text{-cone property}\}. \tag{59}$$

Thus, the following existence result holds:

Theorem 2.6. *Let $\varepsilon > 0$ fixed. The problem*

$$\begin{cases} \min J(\Omega) \\ \Omega \in \mathcal{O}_{V_0}^{\varepsilon} \end{cases} \tag{60}$$

where $\mathcal{O}_{V_0}^{\varepsilon}$ is defined in (59), has a solution.

A very close existence theorem is proved in [15] but is stated in an other frame, since is investigated the optimal shape of a pipe. We refer to this paper for a proof of Theorem 2.6. An essential ingredient of this proof is the fact that $\mathcal{O}_{V_0}^{\varepsilon}$ is closed for the Hausdorff topology (see [15, Lemma 2.2]).

2.2. **An augmented Lagrangian algorithm**

2.2.1. *Mathematical tools*

We present in this section an augmented Lagrangian algorithm to optimize the energy dissiptated by a fluid in a dyadic tree with respect to the shape. The descent direction in the main step of this algorithm will be computed thanks to a gradient method, which implies to calculate at each iteration the derivative of our criterion with respect to the domain. We will firstly recall the expression of such a derivative. The details of its calculation are given in [15].

It is possible to define an adjoint state for the system (54), usefull to write the shape derivative in a very usual form (see [13, Theorem 5.9.2]). Let $(\boldsymbol{v}, q)$ be solution (provided always that it exists) of the linearized Navier-Stokes system

$$\begin{cases} -\mu\Delta\boldsymbol{v} + {}^{\top}(\nabla\boldsymbol{u})\cdot\boldsymbol{v} - \nabla\boldsymbol{v}\cdot\boldsymbol{u} + \nabla q = -2\mu\Delta\boldsymbol{u} & x \in \Omega \\ \nabla\cdot\boldsymbol{v} = 0 & x \in \Omega \\ \boldsymbol{v} = \boldsymbol{0} & x \in E \cup \Gamma \\ -q\boldsymbol{n} + 2\mu\varepsilon(\boldsymbol{v})\cdot\boldsymbol{n} + (\boldsymbol{u}\cdot\boldsymbol{n})\boldsymbol{v} - 4\mu\varepsilon(\boldsymbol{u})\cdot\boldsymbol{n} = 0 & x \in S. \end{cases} \tag{61}$$

The following existence and uniqueness result is established in [15, Proposition 3.1]:

Proposition 2.7. *Let Ω be a bounded Lipschitz domain of $\mathbb{R}^3$. If the viscosity μ is large enough, then the problem (61) has a unique solution $(\boldsymbol{v}, q)$. Moreover, this solution belongs to $(\mathrm{H}^1(\Omega))^3 \times \mathrm{L}^2(\Omega)$.*

Remark 2.8. The variational formulation of problem (61) writes

$$\begin{cases} \text{Find } (\boldsymbol{v}, q) \in W_0(\Omega) \text{ s.t. } \forall (\boldsymbol{w}, \psi) \in W_0(\Omega), \\ \displaystyle\int_{\Omega} (2\mu\varepsilon(\boldsymbol{v}) : \varepsilon(\boldsymbol{w}) + \nabla\boldsymbol{w}\cdot\boldsymbol{u}\cdot\boldsymbol{v} + \nabla\boldsymbol{u}\cdot\boldsymbol{w}\cdot\boldsymbol{v} - q\nabla\cdot\boldsymbol{w})\,\mathrm{d}x = 4\mu\int_{\Omega}\varepsilon(\boldsymbol{u}) : \varepsilon(\boldsymbol{w})\mathrm{d}x \\ \displaystyle\int_{\Omega}\psi\nabla\cdot\boldsymbol{v}\mathrm{d}x = 0. \end{cases} \tag{62}$$

We are now in position to define the derivative of J with respect to the domain. Let us consider a regular vector field $\boldsymbol{V} : \mathbb{R}^3 \to \mathbb{R}^3$ with compact support which does not meet neither E nor S. For small t, we define $\Omega_t = (I + t\boldsymbol{V})\Omega$, the image of Ω by a perturbation of identity and $f(t) := J(\Omega_t)$. We recall that the shape derivative of J at Ω with respect to $\boldsymbol{V}$ is $f'(0)$. We will denote it by $\mathrm{d}J(\Omega; \boldsymbol{V})$. To compute it, we first

need to compute the derivative of the state equation. We use here the classical results of shape derivatives as in [13], [23], [25]. The derivative of $(\boldsymbol{u}, p)$ is the solution of the linear system

$$\left\{\begin{array}{ll} -\mu\Delta\boldsymbol{u'} + \nabla\boldsymbol{u}\cdot\boldsymbol{u'} + \nabla\boldsymbol{u'}\cdot\boldsymbol{u} + \nabla p' = 0 & x\in\Omega \\ \nabla\cdot\boldsymbol{u'} = 0 & x\in\Omega \\ \boldsymbol{u'} = \boldsymbol{0} & x\in E \\ \boldsymbol{u'} = -\dfrac{\partial\boldsymbol{u}}{\partial\boldsymbol{n}}(\boldsymbol{V}\cdot\boldsymbol{n}) & x\in\Gamma \\ -p'\boldsymbol{n} + 2\mu\varepsilon(\boldsymbol{u'})\cdot\boldsymbol{n} = 0 & x\in S, \end{array}\right. \tag{63}$$

where $\boldsymbol{u}$ is, under assumptation that μ is large enough, the unique solution of (54).

Now, we have (see [13], [25])

$$\mathrm{d}J(\Omega;\boldsymbol{V}) = 4\mu\int_\Omega \varepsilon(\boldsymbol{u}):\varepsilon(\boldsymbol{u'})\mathrm{d}x + 2\mu\int_\Gamma |\varepsilon(\boldsymbol{u})|^2(\boldsymbol{V}\cdot\boldsymbol{n})\mathrm{d}s. \tag{64}$$

Using the adjoint state (61), it is possible to rewrite $\mathrm{d}J(\Omega,\boldsymbol{V})$ in a more workable form (see [15, Proposition 3.2]),

$$\mathrm{d}J(\Omega;\boldsymbol{V}) = 2\mu\int_\Gamma \left(\varepsilon(\boldsymbol{u}):\varepsilon(\boldsymbol{v}) - |\varepsilon(\boldsymbol{u})|^2\right)(\boldsymbol{V}\cdot\boldsymbol{n})\mathrm{d}s. \tag{65}$$

Let us now introduce the shape gradient of the criterion J as a functional defined on the boundary and such that $\mathrm{d}J(\Omega;\boldsymbol{V}) = \int_\Gamma \nabla J(\Omega)\cdot\boldsymbol{V}\mathrm{d}s$, in other words

$$\nabla J(\Omega) := 2\mu\left(\varepsilon(\boldsymbol{u}):\varepsilon(\boldsymbol{v}) - |\varepsilon(\boldsymbol{u})|^2\right)\boldsymbol{n}. \tag{66}$$

2.2.2. *Some basic principles on the augmented Lagrangian methods in shape optimization*

We firstly recall the general definition of the augmented Lagrangian and its expected properties in an optimization process. Then, we will give its expression in the case of the problem (58). For a more complete description of such a method in optimal design, one can refer to [2].

Let D be a subdomain of $\mathbb{R}^3$ and E be a set of subdomains contained in D. Let $J : E \to \mathbb{R}$ a functional to be optimized under constraints. We write the shape optimization problem under the form

$$\left\{\begin{array}{l} \min J(\Omega) \\ \Omega\in E_{\mathrm{ad}} := \{\Omega\in E \mid G(\Omega)\in -K\}, \end{array}\right. \tag{67}$$

where $G : E \to Y$ is a functional, Y a Banach space and K a closed convex cone of Y. Y' denotes as usually the topological dual of Y and $\langle .,.\rangle_{Y',Y}$ the duality pairing in Y'. We denote by K^+ the positive dual cone of K, *i.e.*

$$K^+ := \{\mu\in Y' \mid \langle\mu, y\rangle_{Y',Y}\geq 0,\ \forall y\in K\}.$$

Let us assume from now that Y is a Hilbert space, which allows to identify Y and Y' on the one hand, and the duality pairing with the inner product $\langle .,.\rangle$ on Y on the other side. Let $b > 0$ be a parameter. The augmented Lagrangian of the problem (67) associated to parameter b is the functional $\mathcal{L}_b$ defined by

$$\begin{array}{rccl} \mathcal{L}_b: & E\times Y' & \longrightarrow & \mathbb{R} \\ & (\Omega,\mu) & \longmapsto & \mathcal{L}_b(\Omega,\mu) = J(\Omega) + \zeta_b(G(\Omega),\mu), \end{array} \tag{68}$$

where ζ_b is the so-called Moreau-Yosida regularization of $\langle .,y\rangle$, defined for all $y\in Y$ and $\mu\in Y'$ by

$$\zeta_b(y,\mu) = \sup_{\mu'\in K^+}\left(\langle\mu', y\rangle_{Y',Y} - \frac{1}{2b}\left\|\,\mu-\mu'\,\right\|^2_{Y'}\right). \tag{69}$$

One of the main interest of the augmented Lagrangian in comparison with the classical Lagrangian, comes from the fact that the regularization operation improves in general the condition number of the dual function. A faster convergence of the Lagrange multipliers maximizing sequence is then expected. One of the numerical problems arising with the augmented Lagrangian methods is the choice of a correct parameter b, which appears sometimes very difficult to find. We will say a word on this difficulty in 2.2.3.

2.2.3. *The algorithm*

Let us denote by ϖ_{K^+} the projection operator on the convex cone K^+, then the augmented Lagrangian algorithm writes

The augmented Lagrangian algorithm

(1) *Initialization.* Choose $\Omega_0 \in E$ and $\mu_0 \in K^+$.
Let us also fix $\tau > 0$ and $\varepsilon_{\text{stop}}$.
(2) *Iteration k.* We look for a domain Ω_{k+1} such that

$$\begin{cases} \mathcal{L}_b(\Omega_{k+1}, \mu_k) < \mathcal{L}_b(\Omega_k, \mu_k) \\ \Omega_{k+1} \in E. \end{cases}$$

Let $\mu_{k+1} = \mu_k + \frac{\tau}{b}[\varpi_{K^+}(\mu_k + bG(\Omega_{k+1})) - \mu_k]$.
(3) *Stopping criterion.* If $\left\| \mu_{k+1} - \mu_k \right\| \leq \varepsilon_{\text{stop}}$, the algorithm stops. Else, we come back to the previous step.

Furthermore, in the special case of the problem (58), one has $K = \{0\}$, $Y = K^+ = \mathbb{R}$, $\varpi_{K^+} = I$, $G(\Omega) = \text{meas}(\Omega) - V_0$ and the expression of the augmented Lagrangian is

$$\mathcal{L}_b(\Omega, \mu) = J(\Omega) + \mu G(\Omega) + \frac{b}{2} \left(G(\Omega)\right)^2. \tag{70}$$

It is then easy to determine the shape derivative of $\mathcal{L}_b$. One has

$$\mathrm{d}\mathcal{L}_b(\Omega; \boldsymbol{V}) = \int_\Gamma \left[2\mu \left(\varepsilon(\boldsymbol{u}) : \varepsilon(\boldsymbol{v}) - |\varepsilon(\boldsymbol{u})|^2\right) + \mu + b(\text{meas}(\Omega) - V_0)\right] (\boldsymbol{V}.\boldsymbol{n})\mathrm{d}s. \tag{71}$$

We give now some precisions on the second step of the augmented Lagrangian algorithm, in particular on the choice of the descent method. Let Ω_k be the domain obtained at iteration $k-1$, Γ_k its lateral boundary and μ_k the associated Lagrange multiplier. Ω_{k+1} is searched as a perturbation of the identity. That is why we write $\Omega_{k+1} = (I + \varepsilon_k \boldsymbol{d_k})(\Omega_k)$, where $\boldsymbol{d_k}$ is a vector field representing the perturbation of the mesh and ε_k a variable step.

Since we want to implement a gradient method, a first idea would consist in finding $\boldsymbol{d_k}$ verifying

$$\boldsymbol{d_k}_{|\Gamma_k} = -\nabla \mathcal{L}_b(\Omega_k, \mu_k), \ \forall k \in \mathbb{N}. \tag{72}$$

This question has been much studied (see foor instance [1, 22]). In particular, in [10], the authors study similar methods applied to image segmentation, and exhibit some situations in which the choice of $\boldsymbol{d_k}$ as in (72) is numerically the worst solution.

To be more precise, we would like to choose $\boldsymbol{d_k}$ as the solution (if it exists) of the following equation, written under variational form

$$b_k(\boldsymbol{d_k}, \boldsymbol{w}) = -\int_{\Gamma_k} \nabla \mathcal{L}_b(\Omega_k, \mu_k) \cdot \boldsymbol{w}\mathrm{d}s, \ \forall \boldsymbol{w} \in B(\Omega_k), \tag{73}$$

where $b_k(\cdot,\cdot)$ is a inner product and $B(\Omega_k)$ the Hilbert space induced by $b_k(\cdot,\cdot)$. Then we would obviously have

$$0 \leq b_k(\boldsymbol{d_k}, \boldsymbol{d_k}) = -\int_{\Gamma_k} \nabla \mathcal{L}_b(\Omega_k, \mu_k) \cdot \boldsymbol{d_k} \mathrm{d}s = -\langle \mathrm{d}\mathcal{L}_b(\Omega_k, \mu_k), \boldsymbol{d_k}).$$

That is easy to see that choosing $\boldsymbol{d_k}$ as in (72) is the case where $b_k(\cdot,\cdot)$ coincides with the inner product of $\mathrm{L}^2(\Omega_k)$. In this paper, we make the choice of considering $b_k(\cdot,\cdot)$ coinciding with the $\mathrm{H}^1(\Omega_k)$ inner product (see for instance [10] for a mathematical justification). Then, $\boldsymbol{d_k}$ is the solution of the equation

$$\langle \boldsymbol{d_k}, \boldsymbol{w} \rangle_{\mathrm{H}^1(\Omega_k)} = -\int_{\Gamma_k} \nabla \mathcal{L}_b(\Omega_k, \mu_k) \cdot \boldsymbol{w} \mathrm{d}s, \ \forall \boldsymbol{w} \in B(\Omega_k), \tag{74}$$

where $B(\Omega_k) := \{\boldsymbol{w} \in \mathrm{H}^1(\Omega_k) \mid \boldsymbol{w}_{|_{E \cup S}=0}\}$. Indeed, since E and S are the fixed parts of the geometry, the displacement on them has to be null. It is then very classical, using Lax-Milgram's lemma, to see that the problem (74) has a unique solution, which is in $(\mathrm{H}^2(\Omega_k))^3$.

Let us now find the explicit partial differential equation governing $\boldsymbol{d_k}$. Using the Green's formulae, one has for $(\boldsymbol{w}, \boldsymbol{y}) \in [(\mathrm{H}^1(\Omega_k))^3]^2$,

$$\begin{aligned} \langle \boldsymbol{y}, \boldsymbol{w} \rangle_{(\mathrm{H}^1(\Omega_k))^3} &= \int_{\Omega_k} \nabla \boldsymbol{y} : \nabla \boldsymbol{w} \mathrm{d}x + \int_{\Omega_k} \boldsymbol{y} \cdot \boldsymbol{w} \mathrm{d}x \\ &= \int_{\Omega_k} (-\Delta \boldsymbol{y} + \boldsymbol{y}) \cdot \boldsymbol{w} \mathrm{d}x + \int_{\Gamma_k} \frac{\partial \boldsymbol{y}}{\partial \boldsymbol{n}} \cdot \boldsymbol{w} \mathrm{d}s. \end{aligned}$$

As a consequence, $\boldsymbol{d_k}$ is solution of the equation

$$\left\{ \begin{array}{ll} -\Delta \boldsymbol{d_k} + \boldsymbol{d_k} = 0 & x \in \Omega_k \\ \boldsymbol{d_k} = 0 & x \in E \cup S \\ \dfrac{\partial \boldsymbol{d_k}}{\partial \boldsymbol{n}} = -\nabla \mathcal{L}_b(\Omega_k, \mu_k) & x \in \Gamma_k. \end{array} \right. \tag{75}$$

We are now in position to give the complete resolution algorithm of the problem (58).

Resolution algorithm of the problem (58)

(1) *Initialization.* Choose $\Omega_0 \in E$ and $\mu_0 \in \mathbb{R}$.
Let also fix $\tau > 0$ and $\varepsilon_{\text{stop}}$.

(2) *Iteration k.* μ_k is known.

(a) Resolution of the Navier-Stokes problem (and storage of its solution $\boldsymbol{u_k}$)

$$\left\{ \begin{array}{ll} -\mu \Delta \boldsymbol{u_k} + \nabla p_k + \nabla \boldsymbol{u_k} \cdot \boldsymbol{u_k} = 0 & x \in \Omega_k \\ \nabla \cdot \boldsymbol{u_k} = 0 & x \in \Omega_k \\ \boldsymbol{u_k} = \boldsymbol{u_0} & x \in E \\ \boldsymbol{u_k} = 0 & x \in \Gamma_k \\ -p_k \boldsymbol{n} + \mu \varepsilon(\boldsymbol{u_k}) \cdot \boldsymbol{n} = -p_0 . \boldsymbol{n} & x \in S. \end{array} \right.$$

(b) Resolution of the adjoint state (and storage of its solution $\boldsymbol{v_k}$)

$$\left\{ \begin{array}{ll} -\mu \Delta \boldsymbol{v_k} + {}^{\top}(\nabla \boldsymbol{u_k}) \cdot \boldsymbol{v_k} - \nabla \boldsymbol{v_k} \cdot \boldsymbol{u_k} + \nabla q_k = -2\mu \Delta \boldsymbol{u_k} & x \in \Omega_k \\ \nabla \cdot \boldsymbol{v_k} = 0 & x \in \Omega_k \\ \boldsymbol{v_k} = 0 & x \in E \cup \Gamma_k \\ -q_k \boldsymbol{n} + \mu \varepsilon(\boldsymbol{v_k}) \cdot \boldsymbol{n} + (\boldsymbol{u_k} \cdot \boldsymbol{n}) \boldsymbol{v_k} - 4\mu \varepsilon(\boldsymbol{u_k}) \cdot \boldsymbol{n} = 0 & x \in S. \end{array} \right.$$

(c) Calculation of the scalar

$$\begin{aligned}\beta_k &:= \nabla \mathcal{L}_b(\Omega_k, \mu_k) \cdot \boldsymbol{n} \\ &= 2\mu \left(\varepsilon(\boldsymbol{u_k}) : \varepsilon(\boldsymbol{v_k}) - |\varepsilon(\boldsymbol{u_k})|^2\right) + \mu_k + b\,(\text{meas }(\Omega_k) - V_0)\,.\end{aligned}$$

(d) Determination of the displacement direction of the mesh $\boldsymbol{d_k}$, as the solution of the elliptic equation

$$\begin{cases} -\Delta \boldsymbol{d_k} + \boldsymbol{d_k} = 0 & x \in \Omega_k \\ \boldsymbol{d_k} = 0 & x \in E \cup S \\ \dfrac{\partial \boldsymbol{d_k}}{\partial \boldsymbol{n}} = -\beta_k \boldsymbol{n} & x \in \Gamma_k. \end{cases}$$

(e) Determination of ε_k, a step making the augmented Lagrangian decreasing (see Remark 2.9).
(f) Determination of the domain Ω_{k+1}: $\Omega_{k+1} = (I + \varepsilon_k \boldsymbol{d_k})(\Omega_k)$.
(g) Reinitializing of the Lagrange multiplier: $\mu_{k+1} = \mu_k + \tau\,(\text{meas }(\Omega_{k+1}) - V_0)$.

(3) *Stopping criterion.* If $|\mu_{k+1} - \mu_k| \leq \varepsilon_{\text{stop}}$, the algorithm stops. Else, we come back to step (2).

Remark 2.9. Let us say one word on the determination of the variable step ε_k. We use a basic rule in order to avoid too many solving of Navier-Stokes problems at each step.

We start by chosing $\varepsilon_k = \varepsilon_{k-1}$, then

(1) while $\mathcal{L}_b((I + \epsilon_k \boldsymbol{d_k})(\Omega_k), \mu_k) \geq \mathcal{L}_b(\Omega_k, \mu_k)$ we diminish the step by the operation $\varepsilon_k \leftarrow \varepsilon_k/2$.
(2) when a satisfying value for ε_k is found, we go on to the next iteration $k+1$.

Of course, the cost of such a method is quite high since a Navier-Stokes like problem can be solved many times at each iteration. Nevertheless, it is necessary to use such a method in order to be sure that the Largangian function is decreasing. Practically, a good choice of the initial step ϵ_0 permits to avoid too much steps for the choice of ϵ_k. Note that if ϵ_k becomes too small, the algorithm stops.

Let us also say a word on the choice of the parameter b for the augmented Lagrangian algorithm. Practically speaking, b has to be chosen neither too big nor too small. Indeed, the biggest is the parameter b, the best is the conditioning of the dual functional giving the constraints and then the convergence of the sequence of Lagrange multipliers. Nevertheless, if b is chosen too big, the conditioning of the primal problem $\min\{\mathcal{L}_b(\Omega, \mu_k), \Omega \in E\}$ deteriorates and its resolution difficulty increases. That is why before running the algorithm, a compromise has to be done and a lot of preliminary tests are needed to find b.

2.3. **Some numerical results**

In this section, we present 2D and 3D numerical implementations of the algorithm presented upwards. The simulations have been obtained thanks to the augmented Lagrangian method described in 2.2.3 and implemented in the software *Comsol Multiphysics*. The 2D algorithm is an easy adaptation of the 3D algorithm presented upwards.

The Navier-Stokes systems and the adjoint state are solved with a direct finite elements method using Lagrange elements which are $P1$ for pressures and $P2$ for velocities. The displacements of the mesh are $P1$. The multifrontal package (UMFPACK) is used to solve the resultant linear system and a modified Newton like method is used to treat the non linear term. At each iteration k, each node of the geometry is perturbated by the discretized operator $(I + \varepsilon_k \boldsymbol{d_k})(\Omega_k)$ (ALE) and it is sometimes necessary to remesh the geometry when the displacement becomes important.

The Reynolds number in the following computations is around 100 and inertial effects are present. We normalize the applications $J(\cdot)$ and $V(\cdot)$ in such a way that $J(\Omega_0) = 1$ and $V(\Omega_0) = 1$. The value of τ was fixed to 0.5 in all the computations.

2.4. Case where Neumann conditions are imposed at the inlet and Dirichlet conditions are imposed at the outlets

In this section, the initial geometry Ω_0 is a bifurcation whose branches are all identical except for the length of the mother branch which is 1.5 the length of the daughter branches, see figure 3 (2D, left image) and figure 5 (3D, left image). The length of the mother branch has been chosen longer to avoid that the flow at bifurcation level interacts too much with the inlet flow. Indeed the algorithm tends to shorten the mother branch and this phenomenon along with inertial effects in the fluid makes the convergence more difficult to reach if the mother branch is too short initially. The angle between two nearby branches is $\pi/3$.

The boundary conditions correspond to that of the case 1.2.5 adapted to the non-linear regime. Thus a parabolic velocity profile is imposed at each outlets (Dirichlet condition) and pressure constraints are imposed at the inlet (Neumann conditions). The pressure imposed at the inlet is 0.

2.4.1. *2D case*

The Lagrange multiplier has been initialized to $\mu_0 = 0.1$ and the step ε_0 to 10^{-5}.

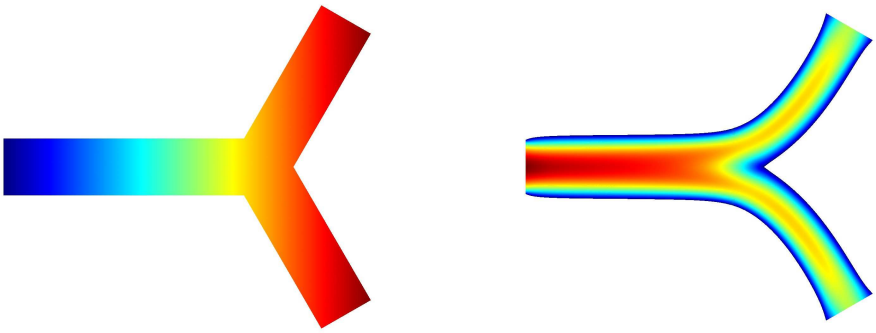

FIGURE 3. 2D Case. Left: initial geometry Ω_0, the inlet is the blue branch while the outlets are the red branches. Right: final shape reached by the algorithm, the colors represent the norm of the velocity u (increasing with the warmth of colors).

The algorithm converges in about 1000 iterations. The final shape of the bifurcation is shown on the right part of the figure 3. The length of the mother branch has shorten and the angle of the bifurcation has become more accute. The diameter of the mother branch has increased while those of the daughter branches have decreased. The convergence of the Lagrange multiplier, of the Lagrangian, of the viscous energy dissipated by the fluid and of the volume of the bifurcation are shown on the figure 4. The viscous energy that the fluid dissipates in the final geometry represents about 80 % of the viscous energy that the fluid dissipates in the initial geometry.

2.4.2. *3D case*

The Lagrange multiplier has been initialized to $\mu_0 = 1$ and the step ε_0 to 10^{-7}.

The algorithm converged in about 1700 iterations. The final shape of the bifurcation is shown on the right part of the figure 5. The results are similar to those in 2D, however the bifurcation in the final shape is closer to the inlet: the length of the mother branch has much more shorten than in 2D and the angle of the bifurcation has thus become more accute than in 2D. The diameter of the mother branch has increased while those of the daughter branches have decreased. The convergence of the Lagrange multiplier, of the Lagrangian, of the viscous energy dissipated by the fluid and of the volume of the bifurcation are shown on the figure 6. The viscous energy that the fluid dissipates in the final geometry represents about 77 % of the viscous energy that the fluid dissipates in the initial geometry.

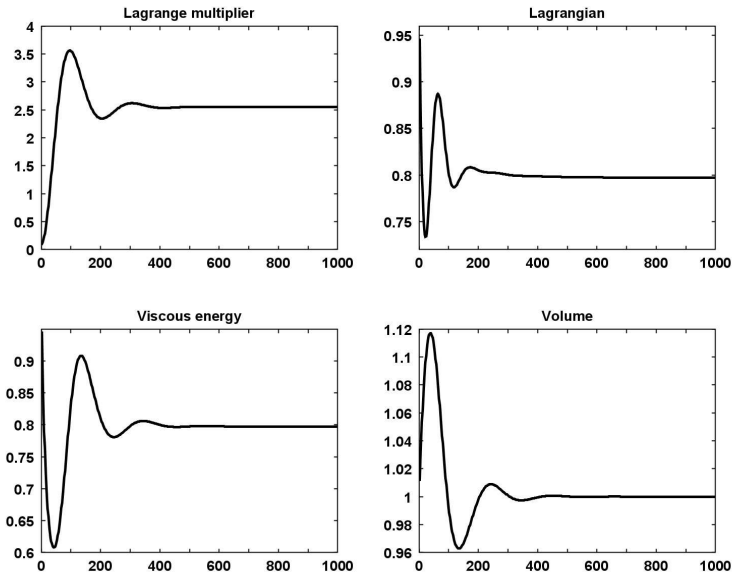

FIGURE 4. 2D case. Convergence curves of the Lagrange multiplier μ_k, the Lagrangian $\mathcal{L}_b(\Omega_k, \mu_k)$, the viscous energy $J(\Omega_k)$ and the volume $V(\Omega_k)$.

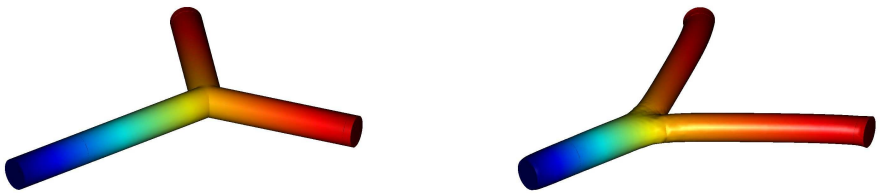

FIGURE 5. 3D case. Left: initial geometry Ω_0, the inlet is the blue branch while the outlets are the red branches. Right: final shape reached by the algorithm.

2.5. **Case where Dirichlet conditions are imposed at the inlet and Neumann conditions are imposed at the outlets**

In this section, the initial geometry Ω_0 is a bifurcation whose branches are all identical, see figure 7 (2D, left image) and 9 (3D, left image). The angle between two nearby branches is $\pi/3$.

The boundary conditions correspond to that of the case 1.2.1 adapted to the non-linear regime. Thus a parabolic velocity profile is imposed at the inlet (Dirichlet condition) and pressure constraints are imposed at the outlets (Neumann conditions). The pressures imposed at the two outlets are slightly different.

These simulations tend to show that the result found theoretically at low regime in section 1.2.1 should also be true for non linear regime.

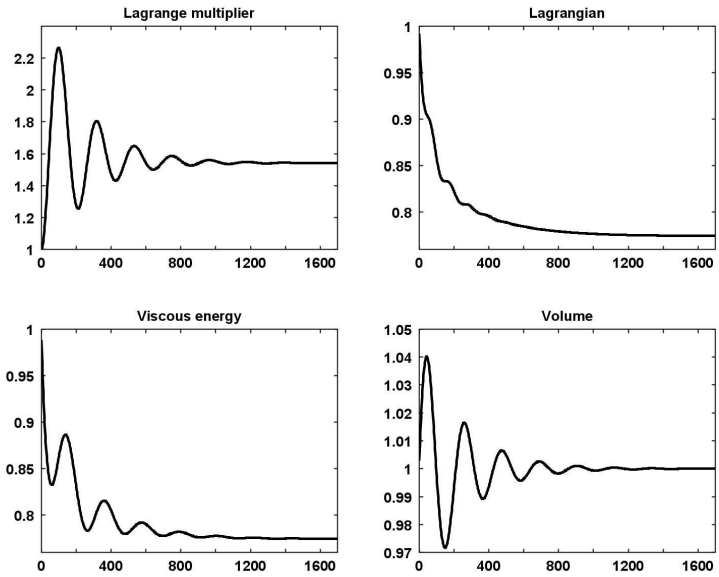

FIGURE 6. 3D case. Convergence curves of the Lagrange multiplier μ_k, the Lagrangian $\mathcal{L}_b(\Omega_k, \mu_k)$, the viscous energy $J(\Omega_k)$ and the volume $V(\Omega_k)$.

2.5.1. *2D case*

The Lagrange multiplier is initialized to $\mu_0 = 0.1$ and the step ε_0 to 10^{-5}.

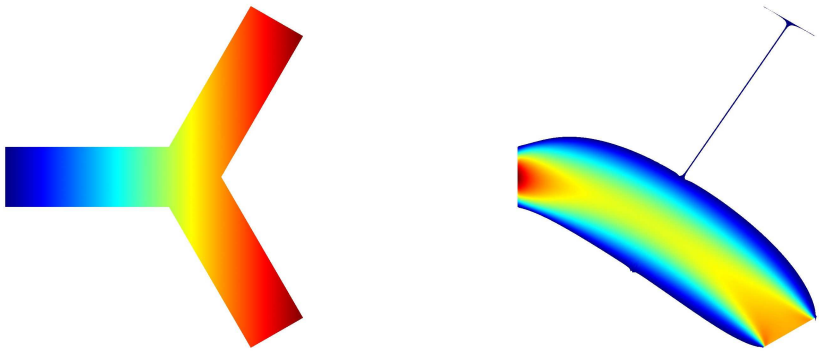

FIGURE 7. 2D case. Left: initial geometry Ω_0, the inlet is the blue branch while the outlets are the red branches. Right: final shape reached by the algorithm, the color represents the norm of the velocity u (increasing with the warmth of colors).

The shape of the bifurcation given by our algorithm is drawn on the right part of figure 7. The final shape is reduced to a simple tube with constant radius. Note that it is slightly rounded because of the different orientations of the inlet and of the outlet that remains open. The algorithm converged in about 2800 iterations. The convergence of the Lagrange multiplier, of the Lagrangian, of the viscous energy dissipated by the fluid and of the volume of the bifurcation are shown on the figure 8. The viscous energy that the fluid dissipates in the final geometry represents about 45 % of the viscous energy that the fluid dissipates in the initial geometry.

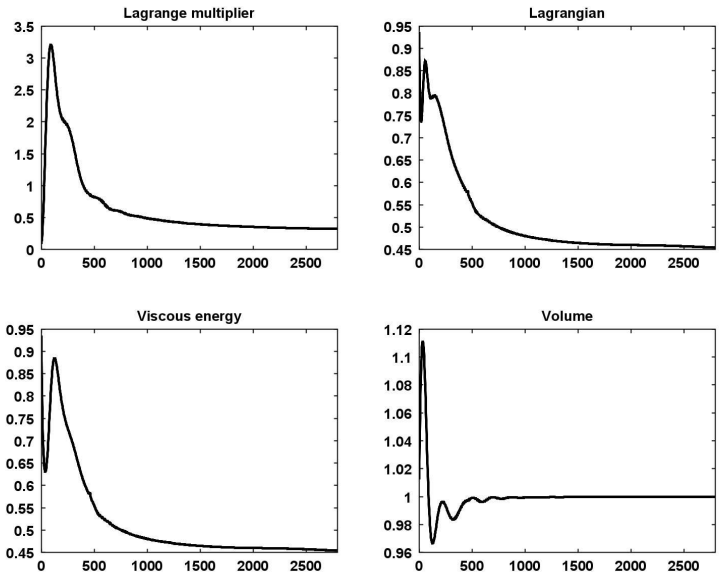

FIGURE 8. 2D case. Convergence curves of the Lagrange multiplier μ_k, the Lagrangian $\mathcal{L}_b(\Omega_k, \mu_k)$, the viscous energy $J(\Omega_k)$ and the volume $V(\Omega_k)$.

2.5.2. *3D case*

The Lagrange multiplier is initialized to $\mu_0 = 0.1$ and the step ε_0 to 5.10^{-8}.

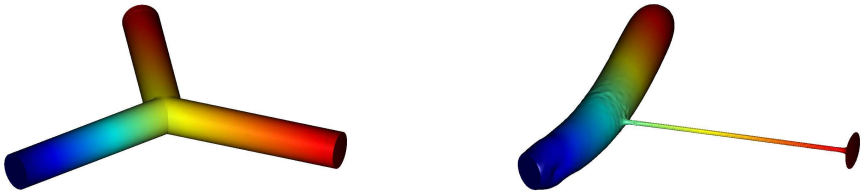

FIGURE 9. Left: initial geometry Ω_0, the inlet is the blue branch while the outlets are the red branches. Right: final shape reached by the algorithm.

The shape of the bifurcation given by our algorithm is drawn on the right part of figure 9. As in 2D, the final shape is also reduced to a simple tube with constant radius. Similarly, it is slightly rounded because of the different orientations of the inlet and of the outlet that remains open. The algorithm converged in about 7000 iterations. The convergence of the Lagrange multiplier, of the Lagrangian, of the viscous energy dissipated by the fluid and of the volume of the bifurcation are shown on the figure 10. One remeshing was needed at the 4500-th iteration to avoid highly deformed elements. This remeshing has induced a slight perturbation in the convergence, see figure 10 where the dashed line marks the step 4500 at which the remeshing was done. The

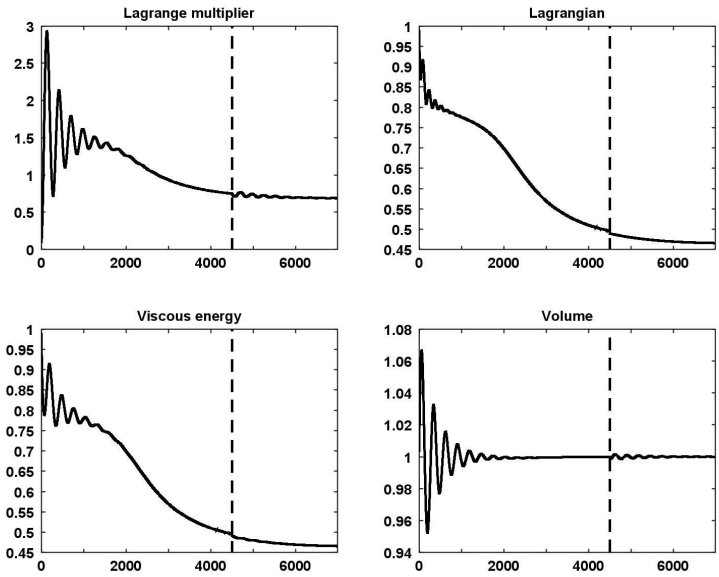

FIGURE 10. Convergence curves of the Lagrange multiplier μ_k, the Lagrangian $\mathcal{L}_b(\Omega_k, \mu_k)$, the viscous energy $J(\Omega_k)$ and the volume $V(\Omega_k)$. The dashed line represents the step 4500 at which a remeshing was done.

viscous energy that the fluid dissipates in the final geometry represents about 46 % of the viscous energy that the fluid dissipates in the initial geometry.

REFERENCES

[1] G. ALLAIRE *Shape optimization by the homogenization method*, Applied Mathematical Sciences, 146, Springer-Verlag, New York, 2002.

[2] S. AMSTUTZ *Augmented Lagrangian for cone constrained topology optimization.*

[3] A. BEJAN, *Shape and Structure, From Engineering to Nature*, Cambridge University Press, Cambridge, UK, 2000.

[4] M. BERNOT, V. CASELLES, J.M. MOREL, *Optimal transportation networks: models and theory*, Vol. 1955 of Lecture notes in mathematics (200 pages), Springer, 2008.

[5] F. BOYER AND P. FABRIE, *Eléments d'analyse pour l'étude de quelques modèles d'écoulements de fluides visqueux incompressibles*, Mathématiques et Applications, 52, Springer-SMAI, 2006

[6] C.-H. BRUNEAU, P. FABRIE, *Effective downstream boundary conditions for incompressible Navier-Stokes equations*, Int. J. for Num. Methods in Fluids, 19, 1994, 8, pp. 693–705

[7] C.-H. BRUNEAU, P. FABRIE, *New efficient boundary conditions for incompressible Navier-Stokes equations: a well-posedness result*, RAIRO Modél. Math. Anal. Numér., 30, 1996, 7, pp. 815–840

[8] D. CHENAIS, *On the existence of a solution in a domain identification problem*, J. Math. Anal. Appl., 52 (1975), 189-289.

[9] M. DELFOUR, J.P. ZOLÉSIO *Shapes and geometries. Analysis, differential calculus, and optimization*, Advances in Design and Control SIAM, Philadelphia, PA, 2001.

[10] G. DOGĞAN, P. MORIN, R.H. NOCHETTO, M. VERANI *Discrete gradient flows for shape optimization and applications*, Computer methods in Applied Mechanics and Engineering, 2007.

[11] G. P. GALDI *An Introduction to the Mathematical Theory of the Navier-Stokes Equations* Volumes 1 and 2, Springer Tracts in Natural Philosophy , Vol. 38, 1998

[12] C. GRANDMONT, B. MAURY, N. MEUNIER, *A viscoelastic model with non-local damping application to the human lungs*, M2AN Math. Model. Numer. Anal., 40(1), 201–224,, 2006

[13] A. HENROT, M. PIERRE, Variation et *Optimisation de forme*, coll. Mathématiques et Applications, vol. 48, Springer 2005.

[14] A. HENROT, Y. PRIVAT, *Une conduite cylindrique n'est pas optimale pour minimiser l'énergie dissipée par un fluide*, C. R. Acad. Sci. Paris Sr. I Math, (2008)

[15] A. HENROT AND Y. PRIVAT, *The optimal shape of a pipe*, to appear in Arch. for Rat. Mech. and Analysis

[16] W.R. Hess, *Das Prinzip des kleinsten Kraftverbrauchs im Dienste h amodynamischer Forschung*, Archiv. Anat. Physiol., 1914.
[17] B. Mauroy, *3D Hydronamics in the upper human bronchial tree: interplay between geometry and flow distribution*, Fractals in Biology and Medicine, IV, 2005
[18] B. Mauroy, *Hydrodynamique dans le poumon, relations entre flux et géométries*, Ph.D. Thesis, ENS Cachan, 2004
[19] B. Mauroy, M. Filoche, J.S. Andrade, B. Sapoval, *Interplay between geometry and flow distribution in an airway tree*, Physical Review Letters, 90, 2003, pp. 1–4
[20] B. Mauroy, M. Filoche, E.R. Weibel, B. Sapoval, *An optimal bronchial tree may be dangerous*, Nature, 427, 2004, pp. 633–636
[21] B. Mauroy, N. Meunier, *Optimal Poiseuille flow in a finite elastic dyadic tree*, M2AN Math. Model. Numer. Anal., 42(4), 2008, pp. 507–533
[22] B. Mohammadi, O. Pironneau, Applied shape optimization for fluids, Clarendon Press, Oxford 2001.
[23] F. Murat, J. Simon, *Sur le contrôle par un domaine géométrique*, Publication du Laboratoire d'Analyse Numérique de l'Université Paris 6, 189, 1976.
[24] Y. Privat, *Quelques problèmes d'optimisation de formes en sciences du vivant*, Ph.D. Thesis Université Henri Poincaré, Nancy, 2008.
[25] J. Sokolowski et J. P. Zolesio, *Introduction to Shape Optimization Shape Sensitivity Analysis*, Springer Series in Computational Mathematics, Vol. 16, Springer, Berlin 1992.
[26] R. Temam *Navier-Stokes Equations*, North-Holland Pub. Company (1979), 500 pages.
[27] D. Tondeur, L. Luo, *Design and scaling laws of ramified fluid distributors by the constructal approach*, Chem.Eng.Sci. , 59, 1799-1813 (2004).
[28] E.R. Weibel, *The Pathway for Oxygen*, Harvard University Press, Cambridge M A, 1984.